Journal of Hydrology 559 (2018) 669–683

Contents lists available at ScienceDirect

Journal of Hydrology

journal homepage: www.elsevier.com/locate/jhydrol

Research papers

Multiple recharge processes to heterogeneous Mediterranean coastal aquifers and implications on recharge rates evolution in time

S. Santoni [a,b,*], F. Huneau [a,b], E. Garel [a,b], H. Celle-Jeanton [c,d]

[a] Université de Corse Pascal Paoli, Faculté des Sciences et Techniques, Laboratoire d'Hydrogéologie, Campus Grimaldi, BP 52, F-20250 Corte, France
[b] CNRS, UMR 6134 SPE, F-20250 Corte, France
[c] Université de Bourgogne Franche-Comté, UFR Sciences et Techniques, 16 route de Gray, F-25030 Besançon Cedex, France
[d] CNRS, UMR 6249 Chrono-Environnement, F-25030 Besançon Cedex, France

ARTICLE INFO

Article history:
Received 22 November 2017
Received in revised form 5 February 2018
Accepted 23 February 2018
Available online 27 February 2018
This manuscript was handled by P. Kitanidis, Editor-in-Chief, with the assistance of Todd C Rasmussen, Associate Editor

Keywords:
Aquifer
Recharge
Rainfall
Hydrochemistry
Stable isotopes
Water management

ABSTRACT

Climate change is nowadays widely considered to have major effects on groundwater resources. Climatic projections suggest a global increase in evaporation and higher frequency of strong rainfall events especially in Mediterranean context. Since evaporation is synonym of low recharge conditions whereas strong rainfall events are more favourable to recharge in heterogeneous subsurface contexts, a lack of knowledge remains then on the real ongoing and future drinking groundwater supply availability at aquifers scale. Due to low recharge potential and high inter-annual climate variability, this issue is strategic for the Mediterranean hydrosystems. This is especially the case for coastal aquifers because they are exposed to seawater intrusion, sea-level rise and overpumping risks. In this context, recharge processes and rates were investigated in a Mediterranean coastal aquifer with subsurface heterogeneity located in Southern Corsica (France). Aquifer recharge rates from combining ten physical and chemical methods were computed. In addition, hydrochemical and isotopic investigations were carried out through a monthly two years monitoring combining major ions and stable isotopes of water in rain, runoff and groundwater. Diffuse, focused, lateral mountain system and irrigation recharge processes were identified and characterized. A predominant focused recharge conditioned by subsurface heterogeneity is evidenced in agreement with variable but highly favourable recharge rates. The fast water transfer from the surface to the aquifer implied by this recharge process suggests less evaporation, which means higher groundwater renewal and availability in such Mediterranean coastal aquifers.

© 2018 Elsevier B.V. All rights reserved.

1. Introduction

Groundwaters represent up to 33% of total water withdrawals around the world and are already widely overexploited (Gleeson et al., 2012; Famiglietti, 2014). Climate spatial–temporal variability and change influences groundwater systems directly through renewal by recharge and indirectly by changes in groundwater use (Taylor et al., 2013a). The renewal of groundwater occurs from many recharge processes which are strongly dependant on climate, land cover and geology (Richts et al., 2011; Jaunat et al., 2016): climate and land cover govern precipitation and evapotranspiration, whereas geology determines water transmission through the soil and storage from the surface and subsurface to aquifers.

Between the global-scale and the basin/site-specific studies connecting groundwater recharge and climatic projections, a lack of knowledge remains concerning the understanding of specific recharge processes within a given region. Since studies of recharge often display different types of recharge, Meixner et al. (2016) defined four main recharge processes to ease comparative analysis in the western United States. Thus, they distinguish diffuse, focused, Mountain System Recharge (MSR) and irrigation recharge. Coupling climate projections with detailed recharge process-based models may thus contribute to reduce aquifer recharge rate estimates uncertainty in predicting aquifer recharge scenarios.

Recently, Hartmann et al. (2017) showed that regions with developed subsurface heterogeneity enhance recharge rates due to a different sensitivity facing climate change compared to more homogeneous regions. According to Hartmann et al. (2017), the concept of heterogeneity refers to hydraulic conductivities, storage capacities and porosities. The ensuing findings indicate that the water balance of Mediterranean and desert heterogeneous areas

* Corresponding author at: Université de Corse Pascal Paoli, Faculté des Sciences et Techniques, CNRS, UMR 6134 SPE, Laboratoire d'Hydrogéologie, Campus Grimaldi, BP 52, F-20250 Corte, France.
E-mail addresses: santoni7@univ-corse.fr, santonisebastien17@gmail.com (S. Santoni).

https://doi.org/10.1016/j.jhydrol.2018.02.068
0022-1694/© 2018 Elsevier B.V. All rights reserved.

will be less dominated by evapotranspiration than regions with homogeneous subsurface because water is rapidly passed downward. To guarantee water resources sustainability, constraining aquifer recharge rates and recharge processes is consequently strategic, especially when recharge conditions are low such as under semi-arid or Mediterranean climate. This is especially the case for coastal aquifers which are highly vulnerable to climate change because exposed to seawater intrusion linked to low recharge conditions, sea-level rise and overpumping risks (Lee et al., 2006; Dhar and Datta, 2009; Javadi et al., 2015).

As a part of the western Mediterranean area considered as a climate change hotspot (Pachauri et al., 2014), the Corsica Island (France) is a strategic place to constrain recharge processes and associated amounts under high climatic pressure. Located at the south of the island, the Bonifacio coastal aquifer has been selected for such a study because the geology and the hydrogeology are well documented and evidenced a noticeable subsurface heterogeneity (McDonnell et al., 2007; Orsini et al., 2010; Reynaud et al., 2012; Santoni et al., 2016a,b,c). In addition, since a MSR and a diffuse recharge have been described in Santoni et al. (2016b) and considering the presence of multiple irrigated vegetable patches, all the 4 recharge processes described previously are suspected to occur at the same time even if the study site is little extended.

Insofar as no seawater intrusion is yet detected in the Bonifacio aquifer (Santoni et al., 2016a), major ions and stable isotopes of the water molecule seemed very suitable to study the recharge because they are able to give insight into the source and timing of recharge (de Vries and Simmers, 2002; Scanlon et al., 2002; Fernandez-Chacon et al., 2010; Florea, 2013). A monthly two years monitoring approach combining major ions and stable isotopes of water in rain, runoff and groundwater was carried out from February 2013 to March 2015 to try to study as accurate as possible the recharge processes.

Aquifer recharge rate estimation are presented from 10 physical and chemical methods for the last three decades before a description of the chemistry and the isotope content in rain, runoff and groundwaters. Then, the recharge processes from hydrochemistry and isotope tools are identified, characterized and prioritized. Finally, the climatic and recharge rates trends are discussed regarding the recharge processes evidenced to infer trends on the ongoing and future water resource availability of Mediterranean coastal aquifers.

2. Study area

2.1. Location and climate

The Bonifacio plateau is located in the southern part of the Corsica Island (Fig. 1). The region is under a typical Mediterranean climate, characterized by highly heterogeneous temperature and rain conditions from one year to another one (Lionello et al., 2006; Bolle, 2012). It is also classified by the Köppen-Geiger criteria

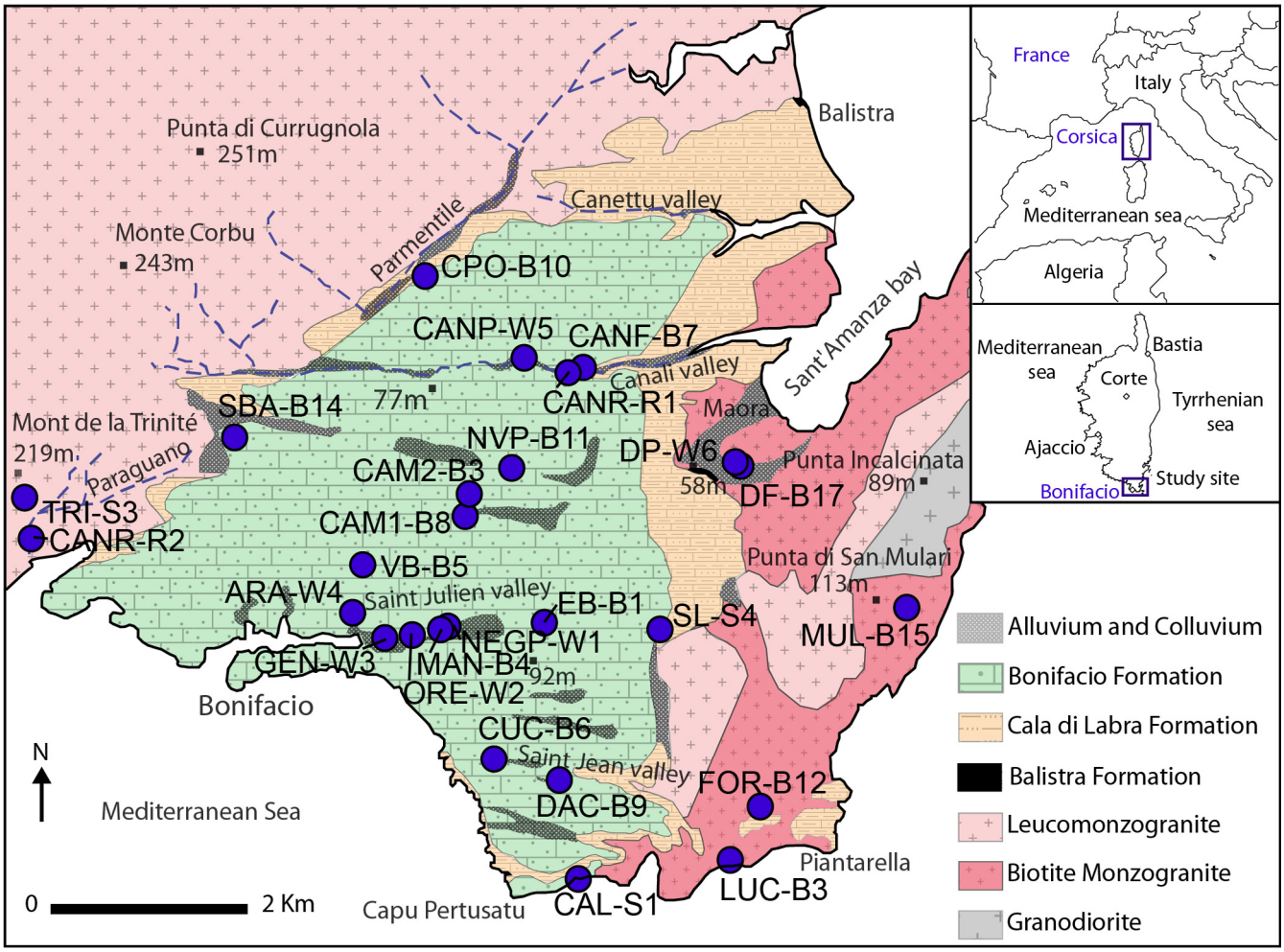

Fig. 1. Location of the study site, general simplified geology from Santoni et al. (2016b) and location of the sampling points.

(Peel et al., 2007) as a so-called "Csa" climate (temperate climate with a dry summer). The mean annual temperature and precipitation at the Bonifacio Météo France station (Capo Pertusato, Fig. 1) are 16.8 °C and 605 mm respectively (calculated from 01/2000 to 01/2012). The sector of Bonifacio is also known for its wind blowing up to 300 days per year, often with gusts above 60–80 km/h, causing heavy swell and generating significant sea sprays all over the region. The study site is bounded in equal proportions by granites at the East and the West, and by the Tyrrhenian Sea at the Northeast and the Mediterranean Sea at the South (Fig. 1). Its triangular shape extends over an area of 25 km2 with a mean elevation of 80 m asl. The Miocene carbonate deposits fill a granitic depression (up to 270 m deep), and are in contact with granitic relief of an altitude up to 243 m at the Monte Corbu (West side) and 113 m at the Punta di San Mulari (East side). The Bonifacio plateau is cut by four East-West oriented valleys: St. Jean, St. Julien, Canettu and Canali. The Canali River is the only permanent river with very low flow during summer and takes its source on the granitic massifs before crossing the plateau in direction of the Sant'Amanza bay. Many streams may appear temporary within the four valleys and also in contact with the granites massifs during high rainfall events. This is especially the case for Paraguano and Parmentile temporary streams located at the North-West interface of the plateau with the granites (Fig. 1). The 3000 inhabitants of Bonifacio reside mainly around the harbour and along the Saint Julien and Saint Jean valleys. Various villas and campgrounds are spread over the plateau. Some scarce agricultural activities like market gardening and cattle breeding are found at the centre of the plateau, the rest of the area being covered by abandoned agricultural land and Mediterranean maquis.

2.2. Geology

The Bonifacio aquifer is developed in a sedimentary Miocene basin and lies on a granitic depression (Fig. 1). From the base to the top, the Bonifacio sedimentary basin is composed of the Balistra (calcareous gravelly sands), the Cala di Labra (shelly litharenites) and the Bonifacio (calcareous fine grained sandy litharenite) formations (Ferrandini, 2003; Orsini et al., 2010; Reynaud et al., 2012). The fraction of calcite also increases to the top of the series as the fraction of weathering products from the surrounding granites decreases. A sandy silt level within the Cala di Labra formation materializes the separation between the upper and the lower aquifer. The granitic bedrock and the sedimentary sequences as a cross section are described in more extended details in Santoni et al. (2016b). The lithology and the structure of the basin suggests clearly a well-developed heterogeneity with respect to porosities and water storage capacities. The granitic bedrock and the Bonifacio basin displays also high heterogeneity due to their intense fracturation: fractures North-South and Northeast-Southwest oriented affects principally the granites, whereas fractures East-West oriented affects both the bedrock and the sedimentary basin (Dörfliger et al., 2002; Gattacceca et al., 2007; Oudet et al., 2010; Reynaud et al., 2012).

2.3. Hydrogeology background

The coastal aquifer hosted by the carbonated sediments represents the only available local groundwater resource in southern Corsica. This region faces also an important touristic activity in summer and additional surface water resources coming from dams located further north are then necessary. The Bonifacio aquifer is composed of two main aquifer levels, separated by the silty layer of the Cala di Labra formation. The thick unsaturated zone up to 50 m in the centre of the plateau is a major characteristic of the aquifer. Environmental tracers allowed assessing mineralization processes and three groundwater types are observed (1) a Ca-HCO_3 water type in the upper aquifer conditioned by carbonate dissolution, (2) a Na-Cl water type in the granites due to sea sprays favoured by the winds, and (3) an intermediate Ca-Na-Cl water type in the lower aquifer conditioned by the mixing of groundwater from the upper aquifer and granites (Santoni et al., 2016a). Some groundwater samples show noticeable nitrate concentrations (up to 40 mg/L) highlighting the vulnerability of the aquifer regarding human activities such as irrigation of gardens and individual sewage treatment plants (ISTP). Groundwater residence time estimations shows weighted ages from 0 to 50 a in the upper aquifer and from 35 to 60 a in the lower aquifer indicating a relatively low dynamic of renewal (Santoni et al., 2016c).

Two flow patterns are identified (1) an autochthonous vertical recharge of the upper aquifer with an aging from the centre of the plateau to the shores (Bonifacio harbour and Sant'Amanza) is observed and consistent with the potentiometric heads and (2) an allochthonous lateral recharge of the lower aquifer *via* the surrounding fractured granites (Santoni et al., 2016c). Hydraulic conductivities range from 1.4 to 2.2×10^{-6} m/s in the upper aquifer and from 2.1 to 4.9×10^{-6} m/s in the lower aquifer (Dörfliger et al., 2002; Santoni et al., 2016c) highlighting the heterogeneity of the aquifer also with respect to hydraulic conductivities. An approach using $^{87}Sr/^{86}Sr$ allowed to validate and compute the mixing rates between the granites, the upper and the lower aquifer. Two outlets are possible for groundwater: (1) anthropogenic, around 180,000 m^3/year of groundwater are taken for drinking water supply needs and (2) natural, through the submarine groundwater discharge (Santoni et al., 2016b). In situ $^{224,223}Ra$ and ^{222}Rn measurements along the coastline display low activities thus reflecting low discharge conditions. The main discharge points were found in the Bonifacio harbour and in Sant'Amanza bay (Fig. 1), in agreement with low temperatures observed using thermal infrared images (Garel et al., 2015).

3. Method

3.1. Aquifer recharge rates estimation

The existing methods in the literature to estimate aquifer recharge rates vary in terms of nature and scale, and includes physical, chemical, isotopic and modelling techniques (Lerner et al., 1990; Hendrickx and Walker, 1997; Zhang and Walker, 1998; Kinzelbach et al., 2002; Scanlon et al., 2002). To achieve realistic estimation and confidence interval, it is strategic to use as much as possible long datasets chronicles and to consider different approaches that complement and support each other (Scanlon et al., 2006). In this way, we computed the aquifer recharge rates from using:

- The ESPERE_v1.5 multiple-method Excel sheet application (Lanini et al., 2016) which allows aquifer recharge rates and aquifer recharge estimations from using several common methods. We applied the empirical methods of Guttman (1947), Turc (1954) and Kessler (1965), the Soil Water Balance methods (SWB) proposed by Thornthwaite (1948), improved by Dingman (2002), and the Water Table Fluctuation (WTF) method proposed by Delin et al. (2007). For the implementation of the ESPERE_v1.5 Excel sheet, we used the daily temperature (°C), daily rainfall amount (mm) and daily potential evapotranspiration (PET, mm) provided by the Météo-France weather station of Bonifacio (Pertusato, Ref. 20041001) for the 01/1980–12/2014 period. The daily water table levels necessary for the WTF method were provided by a OTT Diver CTD device

placed in the borehole CAM2-B3 (recharge area) during the 05/2011–12/2014 period.
- The chloride mass balance (CMB) method was computed for the 01/2013–12/2014 period according to Eriksson and Khunakasem (1969). The mean annual rainfall amount was provided by the Météo-France station of Bonifacio and the monthly chloride concentrations in rainwater and groundwater from the rain gauge and the borehole at CAM2-B3 (recharge area).
- The SAFRAN-ISBA-MODCOU (SIM) hydrometeorological model is provided by Météo France and consists of a combination of a meteorological analysis system (SAFRAN), a land surface model (ISBA), and a hydrogeological model (MODCOU) (Habets et al., 2008). Values for the Bonifacio station were extracted from the Météo-France data base for the 01/2013–12/2014 period.

3.2. Hydrochemistry and isotope composition of waters

3.2.1. Sampling network

Rain, runoff and groundwater from 15 boreholes (up to 270 m deep), 5 wells and 4 springs (Fig. 1) of the surrounding granites, the lower and the upper aquifer levels of the carbonate plateau were monthly sampled from February 2013 to March 2015 for in situ parameters (temperature, pH, electrical conductivity and alkalinity), major ions and $\delta^{18}O$ and $\delta^{2}H$. The screening interval of the boreholes and wells is 31–269 m and 5–15 m respectively. Runoff samples are CANR-R1 and CANR-R2, samples from the upper aquifer in the recharge area are SBA-B14, CPO-B10, CAM2-B3, CANP-W5, NEGP-W1, EB-B1, DAC-B9 and DP-W6, samples from the upper aquifer in the valleys near the outlets are GEN-W3, CUC-B6, CAL-S1, CANF-B7, ARA-W4, VB-B5, ORE-W2, MAN-B4 and NEGF-B16, samples from the lower aquifer are NVP-B11 and CAM1-B8 and samples from the granites are TRI-S3, MUL-B15, FOR-B12, LUC-B13 and DF-B17.

The rainwater sampling has been achieved using a home-made plastic rain gauge as described in Gröning et al. (2012) and placed at the centre of the plateau (near the CAM2-B3 sampling point, Fig. 1). Measurements of physico-chemical parameters and sampling for major ions and for stable isotopes of the water molecule were performed on a monthly basis. The monthly rain amount was also measured in the rain gauge whose max capacity is 275 mm considering the volume of the bottle (25 L) and the funnel surface (908 cm^2). The sampling of unexploited wells and boreholes was performed with a Grundfoss MP1 or a Comet submersible pump depending on the depth of sampling, both with a nylon tube. For exploited ones, water was sampled directly at the tap avoiding any contamination and any air mixing. For sampling points of the upper aquifer, water levels have been measured before pumping. Only 8 sampling points of the upper aquifer guarantee a realistic observation of the water table: CPO-B10, VB-B5, CANF-B7, EB-B1, CAM2-B3, DF-B17, CANP-W5 and MAN-B4.

3.2.2. Analytical procedures

Groundwater Electrical Conductivity (EC) and Temperature (T) were measured in the field with a WTW Cond 3310 m (WTW GmbH, Weilheim, Germany). Bicarbonates were determined in the field using a HACH digital titrator (HACH Company, Loveland, USA). Samples for major ions (Cl^-, SO_4^{2-}, NO_3^-, Na^+, Ca^{2+}, Mg^{2+} and K^+) were filtrated through 0.45 μm nitrocellulose membranes before collection in two 50 mL polyethylene bottles and stored at 4 °C. One of them was acidified using ultrapure HNO_3 for cation analysis. The ionic concentrations were determined with a Dionex ICS 1100 chromatograph (Thermo Fischer Scientific, Waltham, USA) at the Hydrogeology Department of the University of Corsica, France. The chemical analysis quality was checked by computation of the ionic balance error and rejected if >5%. Samples for the stable isotopes of the water molecule analysis were collected in 20 mL amber glass bottles without head-space. The measurements were performed according to the analytical scheme recommended by the International Atomic Energy Agency (Penna et al., 2010) with a liquid–water stable isotope analyser DLT-100 (Los Gatos Research, San Jose, USA) at the Hydrogeology Department of the University of Corsica, France. The isotopic analysis quality was checked with a standard deviation condition up to 1‰ for $\delta^{2}H$ and up to 0.1‰ for $\delta^{18}O$.

3.2.3. Computing procedures

In order to distinguish the sea salt (SS) and the non-sea salt (NSS) ionic fractions in rainwater, the Cl has been assumed as a reference element for sea source (see 3. Method). The sea-salt fractions for any major ion are given by:

$$SS_X = Cl_{RAIN} \times (X/Cl)_{SEAWATER}$$

where $(X/Cl)_{SEAWATER}$ is the standard ratio of the ion X and Cl concentrations from seawater. Non-sea salt fractions for ions X are then computed as:

$$NSS_X = X_{RAIN} - X_{SS}$$

where X_{RAIN} is the concentration of the ion X in rain. The enrichment factors (EF) are also used to identify the sources of ions in precipitation. The EF is computed as follows:

$$EF_X = (X/Cl)_{RAIN}/(X/Cl)_{SEAWATER}$$

If the EF is <1, the enrichment highlights other sources than the marine one. If the reverse appears, the depletion indicates then a loss of ions (Celle, 2000).

The deuterium excess (d-excess) is the enrichment in $\delta^{2}H$ exceeding that of $\delta^{18}O$ occurring principally during evaporation. When precipitation follows the GMWL, the d-excess value is around 10‰ but the relative humidity and temperature of air masses from oceanic origin has a major influence on the initial d composition of water vapour (Merlivat and Jouzel, 1979). It is computed as follows:

$$d\text{-}excess = \delta^{2}H - 8\delta^{1}8O$$

4. Results and discussion

4.1. Aquifer recharge rates estimates

Annual and monthly aquifer recharge rates estimated for the 1980–2014 period are presented in Figs. 2 and 3, respectively. The median annual aquifer recharge rate is about 132 mm (Fig. 2) which corresponds to 26% of the 503 mm of total annual rainfall (Table 1). From one year to another one, the climatic conditions are extremely variable, especially the rainfall amount with values from 279 to 888 mm/year. As a consequence, aquifer recharge rate varies highly and the observed values evolve from 19 to 45% of total annual rainfall, or from 38 to 403 mm/year. The aquifer recharge rates display thus an important inter-annual variability. These observations are very consistent regarding the Western Mediterranean context. As an example, with annual rainfall amounts from 240 mm to 1070 mm, infiltration rates may be <10% in Sardinia and up to 50% in Italy or in Spain (Scozzafava and Tallini, 2001; Ghiglieri et al., 2014; Martos-Rosillo et al., 2015). Karst aquifers from Italy (Sicily), Portugal (Algarve) and Spain (Andalusia) display also wide ranges with infiltration rates between 22% and 67%, whereas porous and alluvial aquifers from Spain (Majorca, Ebro delta), Sardinia or Morocco present values between 9 and 26% (Cimino et al., 1998; Candela et al., 2009; Ghiglieri et al., 2012; Stigter et al., 2014). According to the used

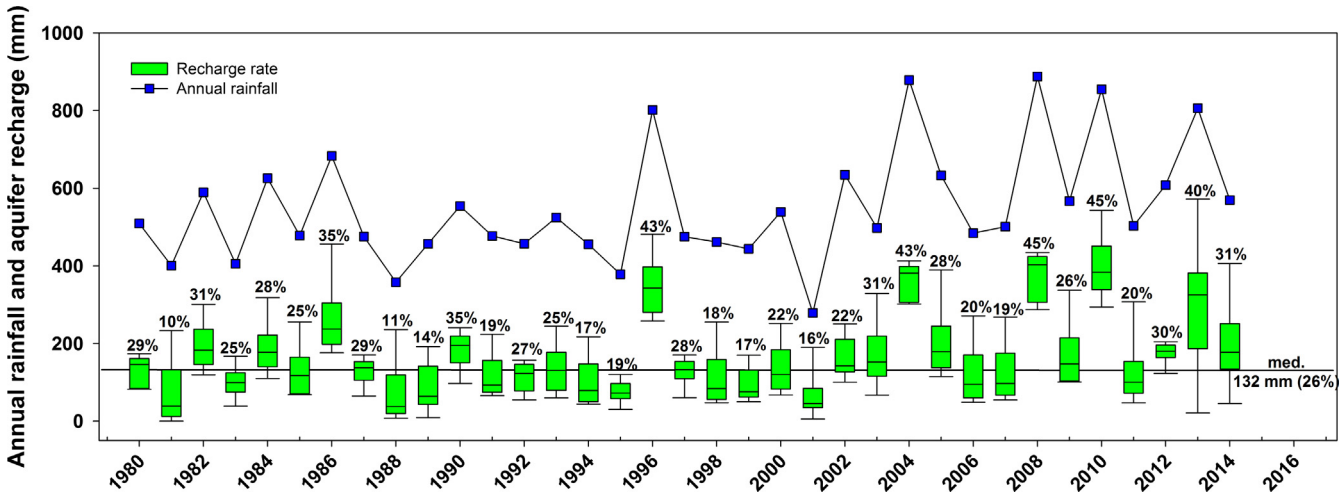

Fig. 2. Annual rainfall and aquifer recharge rate box plots for the 1980–2014 period.

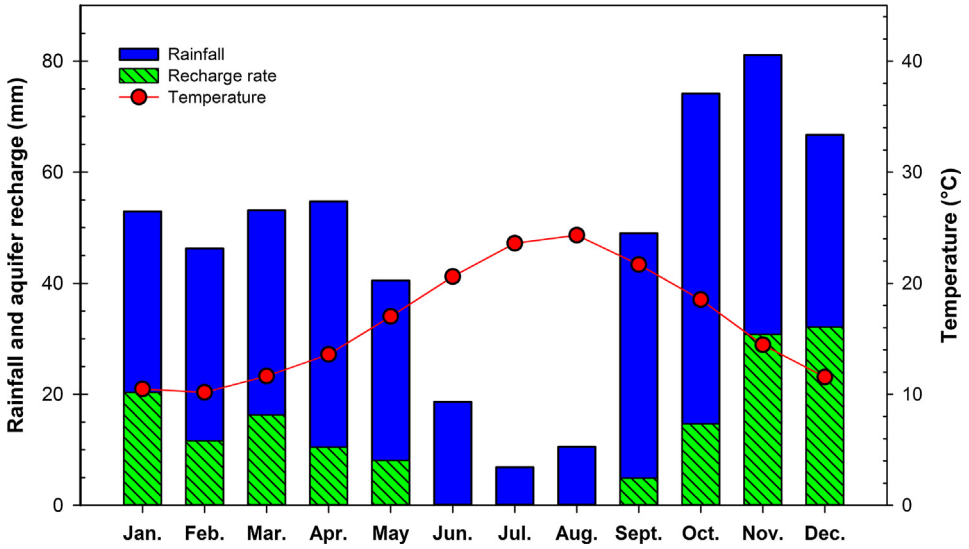

Fig. 3. Temperature, monthly rainfall and aquifer recharge rates means for the. 1980–2014 period.

method, the aquifer recharge rates have a considerable inter-annual and inter-seasonal variability with clear favourable recharge conditions from September to May. The monthly aquifer recharge rates are zero during summer (June, July and August), whereas the maximum are observed during fall-winter with mean values about 30 mm/month for November and December (Figs. 2 and 3). Aquifer recharge rates are noticeable during the winter-spring period, too, with values between 10 and 15 mm/month for the February-May period.

The absolute values of annual aquifer recharge rates nevertheless vary significantly from a method to another one. The Guttman method is supposed to give more realistic results for this study because built on observations from carbonate aquifers under semi-arid climate (Guttman, 1947) similar to the Bonifacio aquifer. The median recharge value about 145 mm thus obtained is very consistent with the values calculated from using the SWB and the WTF methods. Otherwise, the Kessler and SIM methods seem to overestimate the recharge rate with median values about 254 and 355 mm, respectively. The first is more adapted to karstic systems (Kessler, 1965) but remains interesting considering subsurface heterogeneity whereas the latter is rather employed for large scale studies (Habets et al., 2008). The Turc and CMB methods seem for their part to under evaluate the recharge rates with median values about 72 and 34 mm, respectively: the first is limited by considering few parameters (precipitation and temperature; Turc (1954)), and the second is impacted by multiple source and processes affecting chloride concentrations from rainfall to groundwater (Eriksson and Khunakasem, 1969). In any cases, combining all of these methods is the best way to obtain consistent aquifer recharge rate estimations (Scanlon et al., 2006).

4.2. Rainwater characterisation

4.2.1. Rainwater chemistry

The electrical conductivity in Bonifacio rainwater highly varies in time with values between 21 and 343 μS/cm (Table 2) and is well correlated with Na (r = 0.87), Cl (r = 0.75), Ca (r = 0.72) and HCO_3 (r = 0.62). These are also the most abundant elements and represent up to 84% of the total major ions. In order to distinguish the sea salt (SS) and the non-sea salt (NSS) ionic fractions in rainwater, the Cl has been assumed as a reference element for sea source (see 3. Method). All these computations for the monthly Bonifacio rainwater are shown in Table 3. Na, and Mg show EF values around 1, indicating as for Cl, a marine source to their concen-

Table 1
Precipitation, mean annual temperature and aquifer recharge rate estimates from empirical, Soil Water Balance (SWB), Water Table Fluctuation (WTF), Chloride Mass Balance (CMB) and SAFRAN-ISBA-MODCOU (SIM) methods for the 1980–2014 period. Media, mean and standard deviation are given for each year and for each method applied. Annual rainfall amount and mean annual temperature are provided by Météo-France (Pertusato 20041001, Bonifacio climatic station).

Weather data			Aquifer recharge rate (mm)											
Year	Annual rainfall amount (mm)	Mean annual temperature (°C)	Empirical methods			SWB			WTF	CMB	SIM	Median	Mean	Standard deviation
			Guttman	Turc	Kessler	Thorntwaite	Dingman-Penman	Dingman-Hamon						
1980	509	15.3	148	85		82	146	174				146	127	41
1981	401	15.5	99	39	233	0	16	38				39	71	86
1982	590	16.3	184	119	301	155	216	182				183	193	62
1983	405	16.1	101	39	167	87	110	98				100	100	41
1984	626	15.1	190	150	318	110	171	185				178	187	70
1985	478	15.7	134	68	256	72	105	129				117	127	69
1986	683	16.1	240	176	457	206	235	254				238	261	100
1987	476	16.1	133	65	171	119	148	143				138	130	36
1988	358	16.3	80	24	236	7	32	43				38	70	85
1989	457	16.3	125	56	192	9	54	71				64	85	65
1990	554	16.8	168	97	191	212	241	199				195	185	49
1991	477	16.0	134	66	224	80	106	77				93	115	59
1992	457	16.7	125	55	157	121	143	86				123	115	38
1993	525	16.3	155	86	245	60	116	145				131	135	65
1994	456	17.1	124	52	218	44	78	79				79	99	65
1995	378	16.0	89	30	120	67	75	70				73	75	29
1996	802	15.9	345	258	482	288	341	369				343	347	78
1997	475	17.0	133	61	171	132	148	126				133	129	37
1998	462	16.1	127	59	255	47	77	91				84	109	77
1999	444	16.7	119	50	170	66	78	74				76	93	44
2000	539	17.1	162	88	252	68	117	123				120	135	66
2001	279	17.0	45	6	190	45	47	49				46	64	64
2002	635	17.0	198	139	251	100	136	147				143	162	54
2003	498	17.5	143	67	329	132	162	183				153	169	88
2004	879	16.5	413	307	392	302	370	393				381	363	47
2005	633	16.1	196	145	390	115	163	195				179	201	98
2006	485	17.1	137	64	271	49	80	109				95	118	81
2007	501	17.0	145	71	268	54	82	112				97	122	78
2008	888	16.7	421	312	288	387	419	434				403	377	62
2009	567	17.2	174	101	337	104	152	143				148	169	87
2010	855	16.2	392	294	543	354	375	420				384	396	83
2011	503	17.0	145	72	308	47	89	100	154			100	131	87
2012	608	17.1	175	123	180	164	182	204	196			180	175	26
2013	806	16.7	349	252	572	292	325	342	122	21	415	325	299	160
2014	570	17.4	175	101	406	178	208	198	168	46	294	178	197	104
Median	503	16.5	145	72	254	100	143	143	161	34	355	132	131	
Mean	550	16.5	178	108	281	124	158	165	160	34	355	157	167	
Standard deviation	149	0.6	94	82	112	98	102	108	31	18	86			

tration in rainwater. In opposition, HCO_3, NO_3, SO_4, K and Ca displays EF values far higher than 1, signifying that the marine source contributes poorly to their concentration in rainwater. The non-marine source of HCO_3 and Ca about respectively 0.157 and 0.137 meq/L is attributed to the local carbonate dusts from the Bonifacio plateau and may be also attributed to a long distance transport through the sirocco wind (Loye-Pilot et al., 1986). A marine source for Ca is also evidenced with a SS value about 0.011 meq/L. Furthermore, NO_3 and SO_4 about respectively 0.016 and 0.018 meq/l are attributed mainly to anthropogenic atmospheric pollution (Bertrand et al., 2008; Celle-Jeanton et al., 2009) but a marine origin is also highlighted for SO_4 (0.022 meq/L). The Bonifacio rainwaters are consequently under high marine (59%), medium terrigenic (37%) and low anthropogenic (4%) influences. The coastal context of the Bonifacio plateau is obviously the reason why the marine influence is high but this influence is strongly enhanced by the windy conditions causing heavy swell generating significant sea sprays all over the study area. The dry deposits from sea sprays are further solubilized by the rain and then leached through the soil by infiltration waters (Dazy et al., 1997; Alcala and Custodio, 2008; Manca et al., 2015).

4.2.2. Local meteoric water line

The rainfall stable isotope values in Bonifacio for the studied period are between −11.70 ($\delta^{18}O$), −87.4 ($\delta^{2}H$) measured in April 2015 and 2.43 $\delta^{18}O$, 1.9 $\delta^{2}H$ measured in June 2014 and July 2015, respectively. The temporal variation of $\delta^{2}H$ and $\delta^{18}O$ in rainwater depends mainly on climatic factors such as air temperature and humidity, wind speed, evaporation, origin and trajectory of air masses (Rozanski et al., 1982; Clark and Fritz, 1997; Celle-Jeanton et al., 2001). In Bonifacio, the isotope signatures follows naturally a cycle governed by the seasonal climatic variations typically observed in the Mediterranean area (Gat and Carmi, 1970): the most depleted values are mainly found during the winter and the most enriched during the summer (Table 2). The weighted means −6.84‰ for $\delta^{18}O$ and about −44.2‰ for $\delta^{2}H$ are in good agreement with the neighbouring data from Sardinia (Sassari: −6.58‰; −37.3‰) in Longinelli and Selmo (2003) and from Corsica (Ajaccio: −6.89‰; −44.0‰) in Huneau et al. (2015). Due to the Rayleigh distillation process controlling the fractionation of $\delta^{18}O$ and $\delta^{2}H$ (Dansgaard, 1964; Gat and Carmi, 1970), the isotopic content in rainwater usually plot along the global meteoric water line (GMWL) defined by Craig (1961). Nevertheless, the slope may be

Table 2
Physico-chemical parameters, selected major ions and stable isotopes of the water molecule signatures in monthly sampled rainwater.

Sampling date	H (mm)	pH	E. C. (μS/cm)	Na (mg/L)	Cl (mg/L)	Ca (mg/L)	HCO_3 (mg/L)	$\delta^{18}O$ (‰ VSMOW)	$\delta^{2}H$ (‰ VSMOW)	d-excess (‰)
28/02/2013	71.8	7.7	99.0	6.5	4.3	1.1	13.6	−8.64	−53.5	15.7
31/03/2013	140.3	7.4	65.0	3.5	1.9	3.1	15.7	−5.52	−37.2	7.0
30/04/2013	106.1	7.6	36.0	2.9	5.1	2.9	12.9	−5.87	−39.5	7.4
31/05/2013	46.1	6.1	59.0	4.0	7.4	3.6	13.3	−0.03	−8.5	−8.2
01/07/2013	25.9	8.4	21.0	2.1	3.9	1.3	2.9	−4.26	−26.0	8.1
31/07/2013	3	7.2	65.0	2.4	4.3	8.1	16.7	−2.84	−15.2	7.5
05/09/2013	58	8.5	26.0	2.0	3.8	2.1	3.3	−1.44	−12.0	−0.5
30/09/2013	26.6	5.8	63.0	4.8	8.2	2.2	14.3	−3.38	−21.5	5.5
01/11/2013	22.5	7.5	61.0	4.4	2.0	3.8	25.1	−2.50	−12.5	7.5
29/11/2013	177.8	5.9	48.4	6.3	10.5	1.3	4.8	−7.89	−50.9	12.2
03/01/2014	43.8	6.1	103.0	12.0	20.4	3.1	9.1	−8.44	−55.3	12.2
01/02/2014	87.1	5.7	113.0	3.6	26.9	12.9	5.2	−9.05	−61.7	10.7
01/03/2014	70	6.0	50.0	3.9	6.6	1.7	13.5	−6.27	−42.2	8.0
01/04/2014	112.9	7.8	53.0	6.4	11.0	1.5	5.9	−9.71	−65.0	12.7
01/05/2014	44.1	5.9	26.0	2.4	4.1	2.7	9.9	−5.22	−35.6	6.2
04/06/2014	15.9	6.2	117.0	4.8	8.3	11.5	27.2	−1.62	−5.8	7.1
03/07/2014	32.9	8.0	41.2	2.9	5.4	3.8	8.2	2.43	1.6	−17.8
01/08/2014	10.9	7.2	91.0	8.2	13.8	6.7	12.0	−0.03	−8.2	−7.9
30/08/2014	4.8	6.7	198.0	18.2	29.8	7.5	13.8	0.26	1.9	−0.2
02/10/2014	43.8	7.6	21.0	1.1	2.6	1.8	7.3	−4.91	−28.9	10.4
02/11/2014	9.1	5.6	343.0	18.1	33.1	16.1	17.8	−0.82	−5.2	1.3
01/12/2014	74.3	7.3	42.0	3.8	6.4	2.2	4.2	−5.03	−30.4	9.8
05/01/2015	63.8	5.4	45.0	4.6	7.9	1.5	11.5	−8.14	−50.0	15.0
01/02/2015	41.9	7.6	76.0	7.8	12.4	3.6	21.7	−5.11	−29.5	11.3
02/03/2015	112.3	8.5	32.0	3.2	5.4	0.8	6.4	−9.64	−63.2	14.0
03/04/2015	114.3	5.5	33.0	3.0	5.3	1.4	5.7	−7.36	−48.3	10.5
30/04/2015	14.3	7.2	72.0	7.7	13.2	2.9	14.0	−11.70	−87.4	6.2
01/06/2015	9.4	7.4	301.0	8.9	15.2	7.0	47.0	−4.72	−24.2	13.6
02/07/2015	12.3	6.6	80.0	2.7	3.6	7.8	15.0	−1.76	−6.6	7.5

Table 3
Monthly ionic mean concentrations (in meq/L) in the sea and in precipitation with computed sea-source fraction, non-sea-source fraction and enrichment factor (EF) for the 02/2013–03/2015 period.

	HCO3	Cl	NO3	SO4	Na	K	Mg	Ca
Sea	2.712	602.722	0.020	60.586	511.884	8.396	116.942	28.659
Rain	0.158	0.223	0.016	0.041	0.183	0.014	0.047	0.148
X_{SS}	0.001	0.223	0.000	0.022	0.183	0.003	0.043	0.011
X_{NSS}	0.157	0.000	0.016	0.018	0.000	0.011	0.004	0.137
EF	158.1	1.0	2171.9	1.9	1.0	4.7	1.1	14.0

site-specific depending on the local effect of climate and topography (Rozanski et al., 1982; Jaunat et al., 2013; Huneau et al., 2015). The local meteoric water line for the Bonifacio precipitation (BMWL) is defined as $\delta^{2}H = 7.39\ \delta^{18}O + 6.03$ ($r^2 = 0.99$) only considering non-evaporated samples, *i.e.* H > 10 mm and d > 3 (Fig. 4) excluding then the effects of sub-cloud evaporation (Froehlich et al., 2008). This relation is consistent with the Western Mediterranean Meteoric Water Line (WMMWL) of Celle-Jeanton et al. (2001) and with the meteoric water lines of Montpellier, southern France defined as $\delta^{2}H = 7.4\ \delta^{18}O + 7.3$ (Ladouche et al., 2009) or of Sicily, Italy defined as $\delta^{2}H = 6.75\ \delta^{18}O + 8.2$ (Liotta et al., 2013).

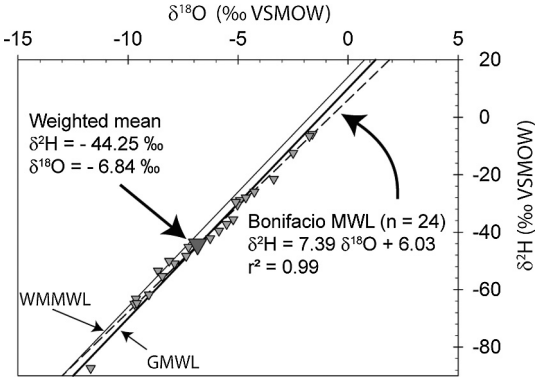

Fig. 4. Rainwater isotopic signatures, weighted mean and Bonifacio meteoric water line (BMWL) from Santoni et al. (2016a) with regard to the Global Meteoric Water Line (GMWL) from Craig (1961) and with regard to the Western Mediterranean Meteoric Water Line (WMMWL) from Celle-Jeanton et al. (2001).

Contributions of recycled moisture evaporated from inland sources conduces usually to lower d-excess values as observed in the Eastern Mediterranean due to a mixing of air masses of North Atlantic and Mediterranean origins (Gat and Carmi, 1987). The low d-excess of 6.03‰ in Bonifacio highlight the importance of the evaporation processes, which may probably be enhanced by strong winds affecting the study site.

4.3. Runoff and groundwater characterisation

Geochemical and isotope analyses of runoff and groundwater appear in Table 4 (mean values). Among all the samples, runoff waters present the highest pH (up to 7.8) and the lowest EC (635 μS/cm), typical of rainwater flowing on carbonates. Moreover, the chloride concentrations in runoff waters (130–145 mg/L) are slightly lower than groundwater (≈230 mg/L) but much higher than rainwater (≈8 mg/L), highlighting a soil leaching of evapo-concentrated sea-salts during surface flow and infiltration (Appelo and Postma, 2005; Meredith et al., 2015). This is also evidenced by the $\delta^{18}O$ whose mean values in runoff (−6.50‰ for PAR-R2; −6.10‰ for CANR-R1) are more enriched than the rainwater

Table 4
Physico-chemical parameters, major ions and stable isotopes of the water molecule mean values and standard deviation (σ) in runoff, groundwater and seawater. The nomenclature is a combination of a lab code and the sampling point type separated by a hyphen (R = Runoff, S = Spring, B = Borehole and W = Well).

Sampling point	Sample origin		T	pH	EC	HCO_3	Cl	NO_3	SO_4	Na	K	Mg	Ca	$\delta^{18}O$	$\delta^{2}H$	d-excess
			°C	–	µS/cm		mg/L							‰ vsmow		
PAR-R2	Runoff	Mean	13.4	7.7	635	83.0	130.4	<0.3	26.4	77.0	2.9	12.6	23.1	−6.50	−39.3	12.4
n = 6		*σ*	*2.3*	*0.4*	*81*	*34.0*	*18.0*	*0.0*	*10.8*	*8.4*	*0.3*	*1.9*	*6.6*	*0.50*	*3.2*	*0.9*
CANR-R1	Runoff	Mean	14.0	7.8	1004	336	145.0	0.5	22.3	82.3	2.2	12.0	111.7	−6.10	−36.6	11.9
n = 25		*σσ*	*4.2*	*0.2*	*254*	*144.7*	*25.0*	*0.3*	*8.8*	*11.4*	*0.6*	*2.3*	*48.6*	*0.50*	*3.3*	*1.5*
EB-B1	UAr	Mean	17.3	7.3	1865	438	326.8	28.7	81.6	150.8	2.8	26.6	205.4	−5.80	−35.0	11.5
n = 24		*σσ*	*1.0*	*0.2*	*159*	*30.8*	*39.3*	*4.3*	*10.0*	*9.6*	*0.5*	*2.3*	*24.7*	*0.20*	*1.0*	*1.2*
CPO-B10	UAr	Mean	17.3	6.7	1889	541	290.9	27.8	60.7	148.8	2.9	21.1	223.2	−6.10	−36.1	12.5
n = 22		*σσσ*	*1.0*	*0.1*	*94*	*63.0*	*33.2*	*8.8*	*6.0*	*13.7*	*0.5*	*1.8*	*17.8*	*0.20*	*1.0*	*1.2*
CAM2-B3	UAr	Mean	18.7	7.0	1126	354	148.1	5.7	29.3	79.2	1.8	9.0	144.8	−5.90	−35.0	12.3
n = 20		*σσ*	*0.8*	*0.2*	*16*	*85.3*	*2.7*	*1.0*	*0.7*	*2.7*	*0.3*	*0.5*	*6.6*	*0.10*	*0.8*	*1.2*
NEG P-W1	UAr	Mean	15.9	7.1	2409	483	452.1	0.1	156.1	231.1	4.6	34.0	227.9	−5.90	−35.7	11.4
n = 11		*σ*	*1.5*	*0.1*	*129*	*15.4*	*39.5*	*0.2*	*17.5*	*15.9*	*1.1*	*0.8*	*10.0*	*0.20*	*0.4*	*1.5*
CANP-W5	UAr	Mean	16.0	7.1	1189	397	160.5	0.4	31.3	96.2	2.3	13.0	133.9	−6.10	−35.9	12.8
n = 15		*σ*	*1.3*	*0.1*	*81*	*27.1*	*25.0*	*0.5*	*4.9*	*12.8*	*0.4*	*1.0*	*6.3*	*0.20*	*0.4*	*1.3*
SBA-B14	UAr	Mean	17.1	7.0	829	324	71.1	13.8	34.7	49.6	3.3	9.1	112.0	−6.20	−37.3	12.2
n = 25		*σ*	*1.1*	*0.2*	*81*	*37.2*	*10.3*	*4.5*	*13.8*	*6.7*	*0.2*	*1.2*	*12.2*	*0.30*	*1.9*	*1.2*
CANF-B7	UAr	Mean	17.9	7.0	1019	379	123.7	3.1	27.3	70.6	3.0	11.5	129.1	−6.20	−36.4	12.9
n = 23		*σ*	*1.1*	*0.2*	*109*	*62.6*	*5.4*	*0.5*	*1.2*	*3.6*	*0.4*	*1.6*	*15.7*	*0.10*	*0.9*	*1.1*
DAC-B9	UAr	Mean	17.8	7.2	1653	357	319.8	5.8	41.7	174.5	4.9	26.2	127.6	−4.90	−30.2	9.4
n = 22		*σ*	*2.0*	*0.1*	*277*	*61.1*	*55.7*	*1.3*	*5.9*	*30.9*	*0.9*	*4.6*	*18.3*	*0.20*	*1.9*	*1.1*
MAN-B4	UAv	Mean	17.8	7.1	1986	448	350.9	18.8	79.4	183.3	6.0	31.5	179.4	−5.80	−34.5	12.0
n = 24		*σ*	*0.5*	*0.2*	*244*	*29.2*	*34.2*	*12.0*	*33.0*	*22.6*	*1.6*	*3.8*	*17.4*	*0.10*	*1.3*	*0.9*
VB-B5	UAv	Mean	18.1	7.3	1112	397	148.5	0.2	1.7	67.5	2.6	11.0	99.5	−6.10	−36.3	12.5
n = 20		*σ*	*1.0*	*0.2*	*35*	*46.0*	*28.8*	*0.2*	*2.3*	*4.5*	*0.3*	*1.0*	*9.7*	*0.10*	*0.9*	*1.2*
CUC-B6	UAv	Mean	18.0	7.2	1267	356	204.7	4.3	31.9	115.8	3.0	16.5	122.5	−5.80	−34.9	11.6
n = 25		*σ*	*0.5*	*0.2*	*13*	*46.8*	*7.8*	*0.7*	*1.1*	*2.7*	*0.4*	*0.7*	*5.5*	*0.10*	*1.0*	*1.4*
NEG F-B16	UAv	Mean	18.4	7.0	1733	207	332.7	8.5	28.1	154.6	9.0	35.9	150.3	−5.70	−33.9	11.9
n = 10		*σ*	*1.3*	*0.2*	*35*	*223.0*	*5.7*	*1.4*	*1.9*	*2.8*	*0.5*	*2.1*	*3.8*	*0.10*	*0.9*	*1.2*
ORE–W2	UAv	Mean	17.6	7.2	1039	335	142.4	4.3	33.9	70.1	2.4	9.5	134.1	−6.10	−36.5	12.1
n = 25		*σ*	*0.6*	*0.2*	*20*	*20.2*	*3.5*	*1.1*	*1.7*	*2.0*	*0.1*	*0.6*	*5.0*	*0.10*	*1.0*	*1.2*
GEN-W3	UAv	Mean	18.5	7.2	1113	385	138.7	4.3	37.6	74.2	4.2	11.1	145.7	−6.10	−36.5	12.6
n = 21		*σ*	*1.1*	*0.2*	*52*	*33.3*	*8.6*	*1.0*	*7.0*	*6.6*	*1.1*	*1.2*	*4.0*	*0.10*	*1.3*	*1.1*
ARA-W4	UAv	Mean	17.8	7.3	1190	387	162.5	11.7	32.6	90.0	2.7	11.8	145.0	−6.20	−37.3	12.6
n = 25		*σ*	*1.0*	*0.3*	*25*	*20.7*	*8.8*	*2.3*	*2.4*	*4.3*	*0.3*	*0.5*	*5.2*	*0.10*	*0.9*	*0.9*
CAL-S1	UAv	Mean	17.2	7.7	1465	356	260.9	2.2	49.8	135.1	3.8	21.0	133.6	−6.20	−36.9	12.6
n = 23		*σ*	*0.6*	*0.2*	*23*	*42.2*	*8.9*	*0.3*	*2.3*	*7.1*	*0.5*	*1.4*	*11.4*	*0.10*	*1.1*	*1.1*
CAL bis-S2	UAv	Mean	17.3	7.6	1473	335	264.2	2.1	47.8	133.0	3.4	21.0	140.6	−6.20	−36.8	12.8
n = 23		*σ*	*0.7*	*0.2*	*52*	*76.4*	*20.1*	*0.3*	*2.0*	*6.9*	*0.4*	*1.4*	*14.2*	*0.10*	*1.0*	*1.3*
CAM1-B8	LA	Mean	18.4	7.0	1087	375	140.9	7.7	26.2	80.0	1.1	9.0	134.4	−6.00	−35.1	12.5
n = 17		*σ*	*0.3*	*0.2*	*15*	*23.5*	*4.7*	*3.2*	*1.7*	*2.5*	*0.1*	*0.6*	*6.5*	*0.10*	*0.8*	*1.1*
NVP-B11	LA	Mean	19.9	7.1	1063	359	138.3	4.4	22.6	86.5	3.4	13.7	115.7	−5.90	−34.1	13.3
n = 12		*σ*	*0.3*	*0.1*	*4*	*18.9*	*12.0*	*0.9*	*0.9*	*1.1*	*0.1*	*0.4*	*2.0*	*0.10*	*0.6*	*0.7*
FOR-B12	G	Mean	17.7	7.4	1712	326	339.6	1.6	73.9	235.7	5.0	26.3	75.2	−5.70	−34.4	11.2
n = 24		*σ*	*1.9*	*0.4*	*418*	*61.7*	*140.8*	*1.3*	*16.6*	*46.4*	*1.5*	*4.8*	*26.2*	*0.20*	*1.5*	*1.2*
LUC-B13	G	Mean	17.6	7.1	2345	255	546.9	0.6	111.7	293.2	5.0	35.4	127.6	−6.30	−37.6	12.5
n = 20		*σ*	*1.9*	*0.2*	*273*	*53.3*	*69.0*	*2.0*	*14.2*	*18.2*	*0.7*	*7.9*	*29.9*	*0.10*	*1.2*	*1.2*
MUL-B15	G	Mean	19.0	6.0	1075	39	268.8	<0.3	50.6	143.5	4.4	24.4	20.9	−6.00	−36.6	11.7
n = 14		*σ*	*0.7*	*0.2*	*483*	*8.5*	*134.3*	*0.0*	*23.1*	*62.9*	*1.1*	*13.1*	*10.0*	*0.20*	*1.7*	*1.1*
DF-B17	G	Mean	17.3	7.3	1617	479	249.1	<0.3	49.8	130.9	3.0	24.2	169.4	−5.90	−34.9	12.6
n = 16		*σ*	*0.5*	*0.5*	*47*	*39.2*	*10.6*	*0.0*	*3.2*	*7.6*	*0.7*	*3.2*	*12.6*	*0.10*	*0.6*	*1.1*
DP-W6	G	Mean	15.6	7.3	1730	500	283.6	<0.3	58.7	152.6	1.8	19.9	188.9	−5.90	−35.3	11.8
n = 25		*σ*	*2.4*	*0.4*	*160*	*42.5*	*58.5*	*0.0*	*13.5*	*13.9*	*0.6*	*2.7*	*21.2*	*0.10*	*0.8*	*1.0*
TRI-S3	G	Mean	18.5	7.0	719	108	143.7	2.3	32.2	86.0	3.9	11.2	35.5	−6.20	−36.5	12.7
n = 25		σ	3.9	0.3	52	37.5	13.4	3.8	5.4	5.1	0.8	2.4	5.3	0.30	1.7	1.1
Seawater	Seawater	Mean	17.9	8.3	57 000	154	21 300	<0.3	2870	11 800	407	1 530	498	1.20	6.9	−2.8
n = 22		σ	4.1	0.3	1	38.9	832.2	0.0	122.6	357.7	155.1	286.2	286.0	0.30	2.1	2.2

weighted mean (−6.84‰). Groundwater of the upper aquifer and especially from the recharge areas shows a wide range of physico-chemical, ionic and isotopic values. This may be evidenced through the EC going from 829 to 2409 µS/cm, the Cl concentration from 71 to 452 mg/L, the HCO_3 from 324 to 541 mg/L, the NO_3 from 0 to 29 mg/L and the $\delta^{18}O$ from -6.2 to -4.9‰. The water types from Ca-HCO_3 to Na-SO_4 and Na-Cl (Fig. 5) reflects also this observation very well.

Groundwater from the granites displays acid to neutral pH (6.0 to 7.4) and highly variable EC, with values from 719 to 2345 µS/cm. As suggested by water types appearing in Fig. 5, the EC is directly influenced by the Na, Cl and K concentrations. The Na and Cl concentrations depend on the distance from the shores through the sea sprays and seawater intrusion. In Table 4, K concentrations around 5 mg/L are induced by groundwater-rock interactions with K-feldspar due to granite weathering (Santoni et al., 2016b). Nevertheless, the highest K concentrations are positively correlated with NO_3 highlighting then a clear anthropogenic vulnerability of recharge waters in some places related to the usage of mineral fertilizers for vegetable patches.

As shown by intermediate physico-chemical, ionic and isotopic values, groundwater from the lower aquifer consists in a mixing of groundwater from the upper aquifer and from the granitic domain. Recharge waters displays then highly variable characteristics due

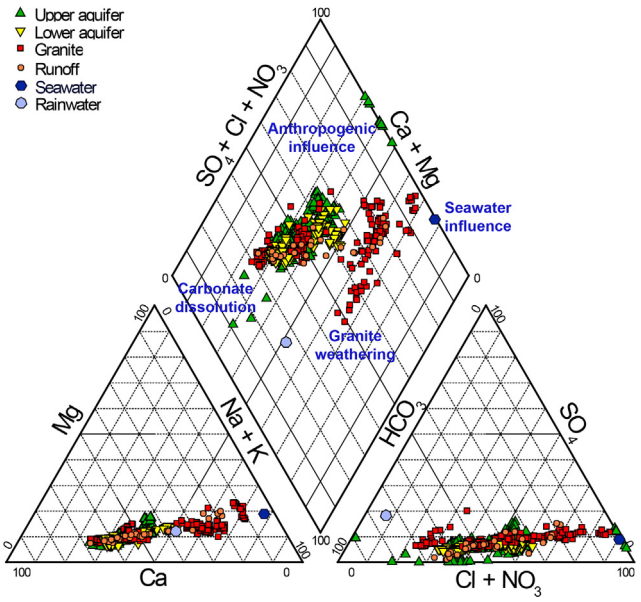

Fig. 5. Piper diagram for all water samples.

to rain and runoff quality variability in time and space, which may also be supported by the existence of multiple recharge processes.

4.4. Recharge processes identification

In order to identify the different recharge processes occurring within the aquifer, box plots were built to illustrate the geochemical and isotopic variations in groundwater over time and space (Fig. 6). Then, the data indicates a clear damping of geochemical and isotopic values from the upper aquifer recharge areas or shallow granitic levels to the upper aquifer outlets, to the deep granitic level and to the lower aquifer. This observation is in very good agreement with the conclusions of Santoni et al. (2016c) showing a low renewal dynamic of the reservoir.

Most groundwater samples are characterized by EC values in the same range than runoff waters, implying a common behaviour for these two water bodies that is only possible by focused recharge (Fig. 6A). The other samples show EC values higher than runoff, sign of other recharge processes occurring.

For the majority of groundwater samples, the nitrate concentrations (Fig. 6B) are under the natural baseline nitrate concentration in the absence of nitrogen fertilization of about 5–7 mg/L (Appelo and Postma, 2005). Nevertheless, the high values (Table 3) observed at some sites are attributed to localized agricultural practices (SBA-B14, EB-B1) or to individual sewage treatment plants (ISTP) such as for CPO-B10. Note that some groundwater samples from the upper aquifer near the outlet shows also noticeable nitrate concentrations (and especially MAN-B4) due to a mixing of old groundwater with a fraction of contaminated recharge water (Santoni et al., 2016c).

The Cl and Na ions are considered here as good tracers of recharge waters because no different source from actual seawater is evidenced (Table 3). Then, some groundwater samples showing Cl concentrations in the same range than runoff waters point to a focused recharge process (Fig. 6C). Otherwise, the sampling point NEGP-W1 being the maximum Cl concentration observed without any seawater intrusion (because of its inland location, the high concentration observed being more related to sea sprays), groundwater samples displaying values higher than these (FOR-B12, LUC-B13) are considered to be potentially mixed with a small seawater fraction. Between these two cases, the groundwater samples displaying Cl concentration above those of runoff and lower than NEGP-W1 are related to soil leaching of evapo-concentrated sea-salts during diffuse infiltration (cf. chapter 4.3) or due to agricultural irrigation return flows and associated evaporation (Chandrajith et al., 2016; Yousif et al., 2016).

The same trend is observed for the $\delta^{18}O$ values (Fig. 6D). Enriched values may reflect irrigation and/or seawater intrusion trends. Moreover, the most ^{18}O depleted groundwater samples find their origin within the surrounding fractured granitic hills where recharge water (MSR recharge process) are influenced by altitude effect (Santoni et al., 2016b). As a consequence, all these observations validate the existence of the four recharge processes described previously (diffuse, focused, MSR and irrigation) within the Bonifacio aquifer.

4.5. Recharge processes characterisation

To characterize the recharge processes, a selection of 3 sampling points located in the recharge area (Fig. 6) and representative of different contexts have been compared with climatic parameters, input signal and runoff (Fig. 7): (1) the sampling point CPO-B10 is considered as representative of groundwater recharged in the valleys by a focused way due to its location near the Parmentile temporary stream and due to the availability of a representative water table level chronicle, (2) the sampling point DP-W6 has been selected to be representative of groundwater recharged by a diffuse way and (3) the sampling point EB-B1 is considered to be representative of groundwater potentially recharged from irrigation. Note that previous studies already defined the presence of MSR recharge process by highlighting a lateral recharge of the carbonate plateau due to a hydraulic connection with the surrounding fractured granites (Santoni et al., 2016b,c).

As described previously, the rainfall scheme displays a strong seasonal evolution with an alternation of dryer periods (end of spring to summer-fall) and wetter periods (fall-winter to the beginning of spring). Most of the time, the difference between the rainfall amount and the PET is negative, which means that the infiltration from rain to the water table is supposed impossible. During high rainfall periods, the difference between the rainfall amount and the PET is positive allowing then recharge processes to be activated (*e.g.* Jan. to Mar. 2013, Nov 2013 to Mar. 2014 and Nov–Dec. 2015). Depending on the prevailing recharge processes, the water flow transfer will result in variable behaviours of the hydraulic charge and also of geochemical and isotopic tracers.

4.5.1. Focused recharge

The focused recharge is defined as recharge from ephemeral or perennial surface-water through concentration of precipitation and runoff processes and resulting infiltration at specific location on the landscape.

The potentiometric level at the sampling point CPO-B10 appears as conditioned by the rainfall scheme, with a continuous decrease starting at the end of spring until the next winter (min. around 70 m a.s.l), before a quick increase few months after the rainiest periods (max. up to 75 m a.s.l). The same trend is observed with the Cl content and with the $\delta^{18}O$ values: their evolution over time is well correlated with the input signal and runoff. Indeed, there is a seasonal variation of the chloride concentration in runoff and groundwater at CPO-B10, with lower values during rainfall periods because of ionic dilution (up to 106 mg/L in runoff, 175 mg/L at CPO-B10) and higher values during wetter periods (up to 176 mg/L in runoff, 355 mg/L at CPO-B10) due to ionic concentration process. Similar variations are observed for $\delta^{18}O$ values with more depleted values during rainfall periods (up to −6.61‰ for

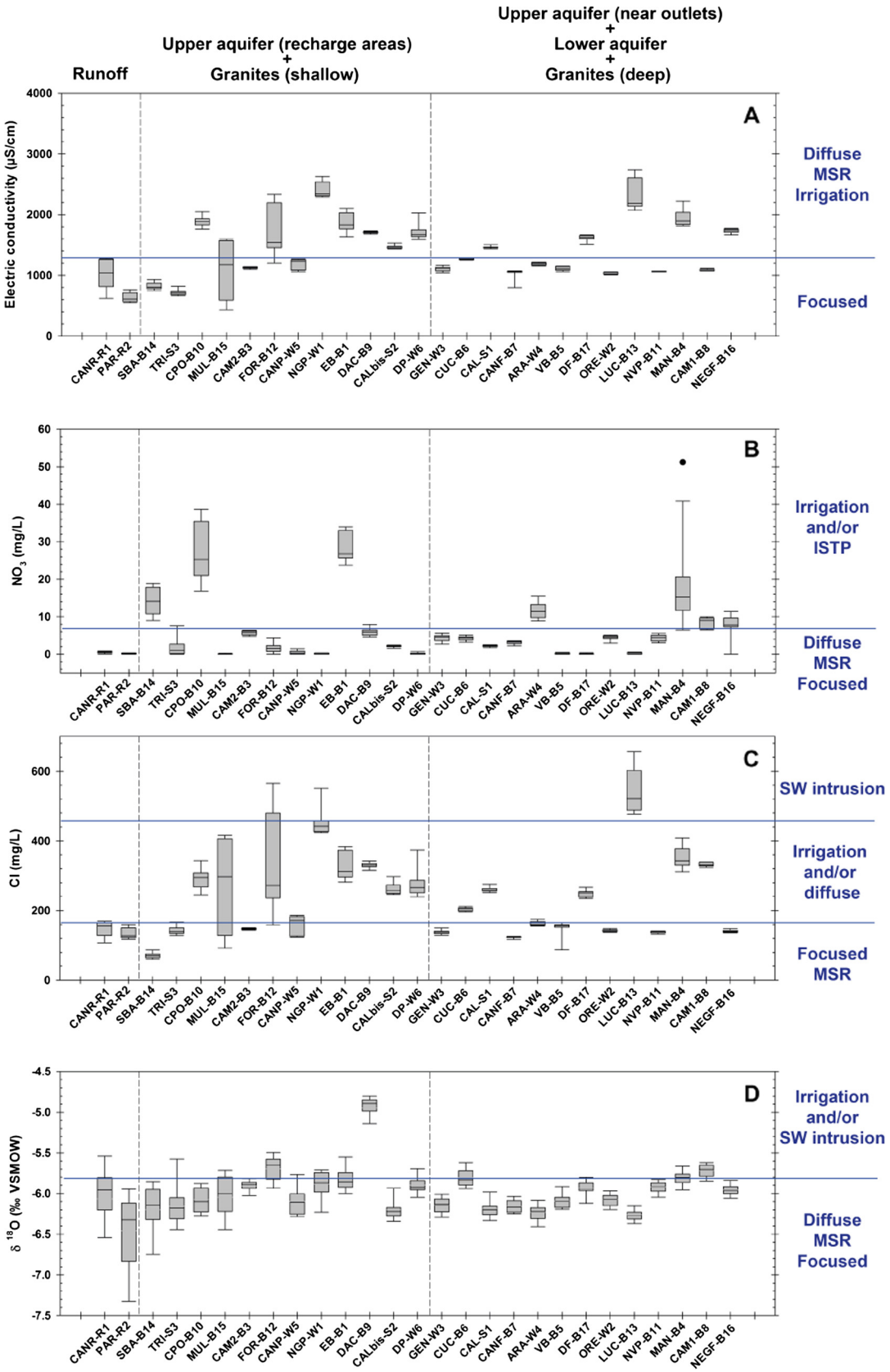
Runoff
Upper aquifer (recharge areas) + Granites (shallow)
Upper aquifer (near outlets) + Lower aquifer + Granites (deep)
A
Electric conductivity (µS/cm)
Diffuse MSR Irrigation
Focused
B
NO3 (mg/L)
Irrigation and/or ISTP
Diffuse MSR Focused
C
Cl (mg/L)
SW intrusion
Irrigation and/or diffuse
Focused MSR
D
δ 18O (‰ VSMOW)
Irrigation and/or SW intrusion
Diffuse MSR Focused
CANR-R1 PAR-R2 SBA-B14 TRI-S3 CPO-B10 MUL-B15 CAM2-B3 FOR-B12 CANP-W5 NGP-W1 EB-B1 DAC-B9 CALbis-S2 DP-W6 GEN-W3 CUC-B6 CAL-S1 CANF-B7 ARA-W4 VB-B5 DF-B17 ORE-W2 LUC-B13 NVP-B11 MAN-B4 CAM1-B8 NEGF-B16

Fig. 6. Box plots from selected physico-chemical parameters, major ions and stable isotopes for all runoff and groundwater samples: (A) is for electric conductivity, (B) for nitrate concentrations (C) for chloride concentrations and (D) for $\delta^{18}O$. MSR: Mountain System Recharge, ISTP: Individual Sewage Treatment Plant, SW: Sea Water.

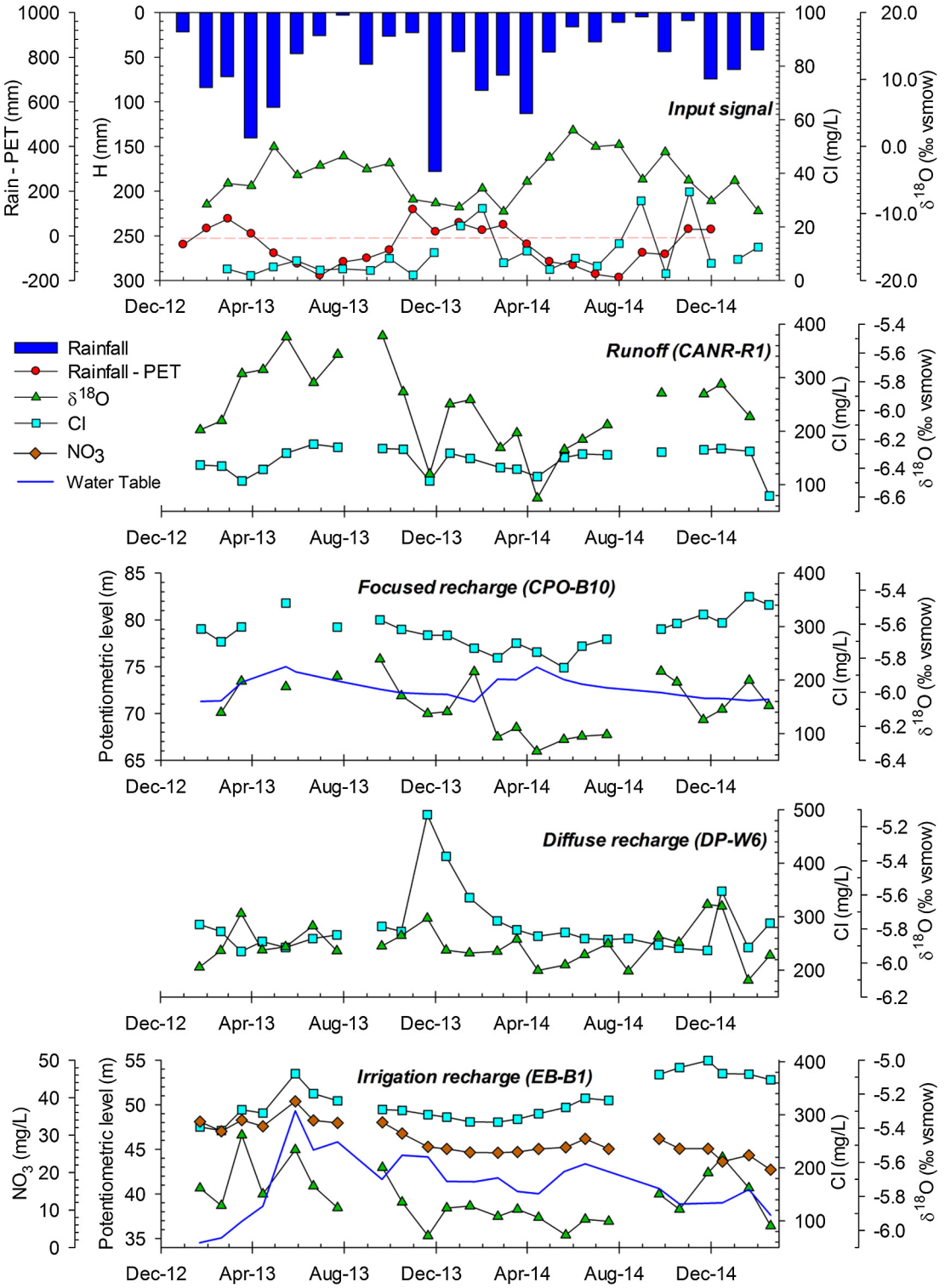

Fig. 7. Monthly rainfall, PET, water table, chloride, nitrate and $\delta^{18}O$ chronicles in rainwater, runoff, focused, diffuse and irrigation recharged waters.

runoff, −6.35‰ at CPO-B10) and more enriched ones during wetter periods due to evaporation processes (up to −5.48‰ in runoff, −5.80‰ at CPO-B10). Information coming from the evolution of water table, chloride and oxygen-18 over time strongly argue in favour of intense runoff-groundwater interactions. This finding is thus synonym of continuous and quality-variable recharge conditions over time, typical of focused recharge.

4.5.2. Diffuse recharge

Diffuse recharge corresponds to recharge waters from precipitation occurring as a direct infiltration of rain followed by percolation to the water table.

The chloride concentrations in groundwater samples from DP-W6 are fairly stable around 280 mg/L. This value is relatively high and may be related to sea sprays due to the vicinity of the shore

(Fig. 1). When the difference between the rainfall amount and the PET turns positive, groundwater from this sampling point displays a quick and intense increase in chloride concentrations with values up to 490 mg/L (November 2013) and up to 347 mg/L (December 2014) before a progressive decrease until the base level concentration. This observation is typical of soil evapo-concentrated sea salt leaching by recharge water (Appelo and Postma, 2005; Meredith et al., 2015). Furthermore, the behaviour of groundwater $\delta^{18}O$ signature over time displays a similar pattern than runoff or focused recharge but with a lower amplitude (from −6.10‰ to −5.66‰) and with a delay of 2–3 months respectively related to a low recharge of inertial water bodies and to the deep unsaturated zone (Santoni et al., 2016c). This finding, associated with water Ca-HCO_3 to Na-Cl water types highlighting both influences of outcropping calcarenites and rainwater influenced by seawater signature (Fig. 5, Table 3) testifies consequently of the presence of diffuse recharge processes.

4.5.3. Irrigation recharge

Irrigation recharge is the water from cropping irrigation that reach the water table and may be derived from surface and groundwater.

The potentiometric level at the sampling point EB-B1 is highly variable (from 29.8 to 49.3 m a.s.l) and is characterized by a succession of seasonal peaks. As expected, some of them are observed during the rainiest periods when the natural recharge processes are activated. Higher levels are additionally observed from the end of spring to the end of summer even if the difference between the rain amount and the PET is negative (*e.g.* May–June 2013, June–July 2014). All these peaks are associated higher concentrations in nitrate (from 20 up to 39 mg/L) and chloride (from 270 up to 402 mg/L) as well as higher $\delta^{18}O$ values (from −5.79 to −5.53‰), especially for the May–June 2013 period. Such solute contents and isotopes ratios enrichments may be due to agricultural irrigation return flows and associated evaporation (Chandrajith et al., 2016). This finding consequently argue in favour of a recharge induced by irrigation.

4.5.4. Lateral recharge (MSR)

The MSR is the recharge provided by streams loss at mountain fronts and resulting sub-surface transfer of groundwater from the mountain block to the adjacent aquifer. The lateral recharge process of the Bonifacio aquifer has been described in previous studies: (1) Dissolved anthropogenic atmospheric gases CFCs and SF_6 were used to evaluate groundwater residence time and flow pattern (Santoni et al., 2016c). Natural SF_6 from pegmatite veins of the surrounding fractured granites found within the carbonate aquifer has been used as a direct tracer of groundwater origin, highlighting a lateral recharge especially for CAM1-B8, NVP-B11 and SBA-B14; (2) An approach coupling the $\delta^{18}O$ and the $^{87}Sr/^{86}Sr$ allowed to compute and validate the mixing rates between the granites, the lower and the upper aquifer (Santoni et al., 2016b). The recharge provided by the neighbouring fractured granites represents up to 24% of the total recharge. This additional natural recharge rises consequently the recharge area of the aquifer of +32% in surface which is now extended to the whole topographic catchment boundaries.

4.6. Identifying the main processes conditioning recharge

The $\delta^{18}O$ vs $\delta^{2}H$ graph (Fig. 8A) is here employed as a tool to deduce groundwater origins. All 511 groundwater samples are plotted on the global, the western Mediterranean and the Bonifacio meteoric water lines. This means that groundwater is actively recharged by modern local precipitation. The groundwater isotopic signatures from −28 to −42‰ and from −6.9 to −4.6‰

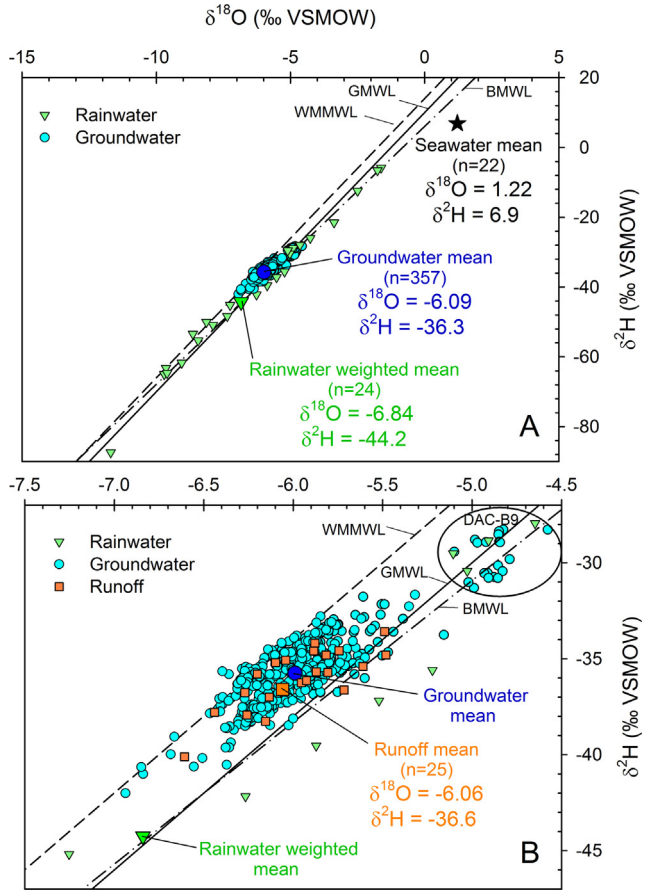

Fig. 8. $\delta^{2}H$ vs $\delta^{18}O$ plots of seawater, rainwater and groundwater with associated means values (A). The graph enlargement displays also the runoff plots and associated means values and the groundwater sampling point DAC-B9 showing a slight fraction of seawater (B).

are significantly different from the signature of seawater with values of about +6.9‰ and +1.22‰ for $\delta^{2}H$ and $\delta^{18}O$, respectively. Consequently, no noticeable seawater intrusion is appearing (except locally and punctually, as for DAC-B9). Nevertheless, there is a difference between the groundwater isotopes mean values of −36.3‰ for $\delta^{2}H$ and −6.09‰ for $\delta^{18}O$ and the rainwater weighted mean values of −44.2‰ for $\delta^{2}H$ and −6.84‰ for $\delta^{18}O$. Usually in such an aquifer, the groundwater isotope value is similar to the weighted mean of the annual rainwater isotopic signature. But the slight isotopic enrichment of groundwater observed here accurately coincides with the runoff mean of −36.6‰ for $\delta^{2}H$ and −6.06‰ for $\delta^{18}O$ (Fig. 8B). Nevertheless, the d-excess being most of the time around 11–13‰ in all groundwater samples, evaporation is not the main process occurring during runoff: the enrichment seems then rather related to a rapid infiltration of rainwater occurring also during winter-spring with less negative isotopic values than fall-winter rainwater (Table 2). Rapid infiltration of runoff waters is realistic taking into account the heterogeneity of the study site described in the study area section. This is also well supported by the median annual aquifer recharge rate about 26% of the 508 mm of total annual rainfall described previously (Fig. 2). This value is indeed relatively high compared to similar carbonate coastal aquifers in the western Mediterranean whose recharge rate is generally from 9 to 18% (Ghiglieri et al., 2014; Stigter et al., 2014). All these conclusions argue strongly in favour of a predominant focused recharge process within the Bonifacio aquifer, on which are superimposed diffuse, MSR and irrigation processes.

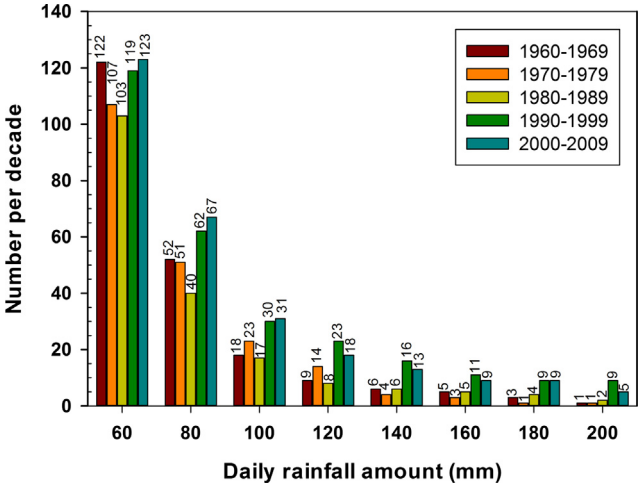

Fig. 9. Amount of the daily rainfall events for the last completed five decades.

4.7. Focused recharge and water resource availability

Recently, evidence of the dependence of groundwater resources on extreme rainfall were made in East Africa (Taylor et al., 2013b). Their groundwater isotope signatures were different from a weighted mean of rainwater due to El Nino Southern Oscillation and Indian Ocean Dipole mode disproportional contribution to recharge, highlighting then the role of extreme rain events favouring aquifer recharge. Since high rainfall events are predicted to be more and more frequent in the Mediterranean (Scanlon et al., 2006), this change in rainfall scheme should have consequences on the aquifers recharge conditions. It appears necessary to evaluate if the Mediterranean climatic trends are verified at the local scale in the present study. In this aim, the number of daily rainfall events per decade for the 1960–2009 period (provided by Météo France) are presented in Fig. 9 for the Southern Corsica area. For rainfall events up to 60 mm/day, no noticeable variation is visible. In contrast, a clear increase in the 80–200 mm/day events appears for the last two decades: as an example, the number of daily rainfall amounts about 100 mm increase from 17 to 23 for the 1960–1989 period to 30–31 for the 1990–2009 period. This is the same for rainfall amounts about 140 mm with an increase from 4 to 6 for the 1960–1989 period to 13–16 for the 1990–2009 period. The global climatic trends implying an increase in high rainfall events are thereby verified at the local scale of the Bonifacio aquifer.

A very good linear correlation is observable between the annual rainfall amounts and the corresponding recharge rates with an r^2 about 0.92. This observation implies that more intense rain events means more favourable recharge conditions. This is well illustrated by the highest recharge rates observed recently (1996, 2004, 2008, 2010 and 2013) with values between 40 and 45% (324–403 mm) of the annual rainfall amount (Fig. 2, Table 1). The authors are aware that by using the ESPERE code, the recharge rate should increase with increased precipitation, but this observation is still realistic since a focused recharge process prevails within the Bonifacio aquifer. Indeed, focused recharge is known to favour aquifer recharge rates in regions with heterogeneous subsurface characteristics because water is rapidly passed downward (de Vries and Simmers, 2002; Scanlon et al., 2002; Meixner et al., 2016; Hartmann et al., 2017).

The present findings indicate that the climate change seems to enhance groundwater availability of such heterogeneous Mediterranean coastal aquifers, as suggested by the projections of Hartmann et al. (2017).

5. Conclusions

The findings of this study clearly demonstrate that the sensitivity of groundwater renewal of Mediterranean coastal aquifers is dependent on the prevailing recharge process.

For the first time, a monthly two years monitoring approach combining major ions and stable isotopes of water in rain, runoff and ground waters allowed to observe and characterize four recharge processes within a heterogeneous coastal aquifer in the Mediterranean area. The groundwater isotopic signatures clearly demonstrate the domination of the focused recharge process on which are superimposed diffuse, MSR and irrigation processes. The very good correlation between the rainfall amount and the recharge rate in Bonifacio implies actually that more intense rain events consequently means more favourable recharge conditions. Rapid infiltration of runoff waters is most likely caused by the surface heterogeneity of the study site. High rainfall events being predicted to be more frequent in the future, focused recharge constitutes thus an important process favouring aquifers recharge in Mediterranean regions with heterogeneous subsurface characteristics.

The findings of the present paper are strategic because coastal aquifers are the most vulnerable hydrosystems to climate change since they are exposed to seawater intrusion which can get worse due to low recharge conditions, sea-level rise and over pumping risks. Better constrained aquifer recharge rates and recharge processes contribute to guarantee the water resources sustainability and availability, especially when recharge conditions are not favourable and highly variable such as under semi-arid or Mediterranean climate. Likely water management strategies including adapted water management plans have to take into account the variable flow dynamics of such aquifers with heterogeneous recharge behaviour. Groundwater pumping rates could be then adapted to the temporally variable water availability. This issue is especially acute in the Mediterranean region, where the expected high inter-annual variability of recharge will require adapted measures for water resources protection and management to use the potential additional recharge evidenced in this study.

Acknowledgement

The Ph.D grant of Sébastien Santoni was financially supported by the Regional Council of Corsica (Collectivité Territoriale de Corse). The authors would like to thank the municipality of Bonifacio for their support and contribution to the implementation of the project. The authors would also like to thank the Bonifacio inhabitants for access to their wells and boreholes during the field sampling. The authors are grateful to M. Patrick Rebillout from Météo France Ajaccio for providing the weather data.

References

Alcala, F.J., Custodio, E., 2008. Atmospheric chloride deposition in continental Spain. Hydrol. Process. 22, 3636–3650. https://doi.org/10.1002/hyp.6965.

Appelo, C., Postma, D., 2005. Geochemistry, Groundwater and Pollution. Taylor & Francispp.

Bertrand, G., Celle-Jeanton, H., Laj, P., Rangognio, J., Chazot, G., 2008. Rainfall chemistry: long range transport versus below cloud scavenging. A two-year study at an inland station (Opme, France). J. Atmos. Chem. 60, 253–271. https://doi.org/10.1007/s10874-009-9120-y.

Bolle, H.-J., 2012. Mediterranean Climate: Variability and Trends pp. Springer Science & Business Media. 410.

Candela, L., von Igel, W., Javier Elorza, F., Aronica, G., 2009. Impact assessment of combined climate and management scenarios on groundwater resources and associated wetland (Majorca, Spain). J. Hydrol. 376, 510–527. https://doi.org/10.1016/j.jhydrol.2009.07.057.

Celle-Jeanton, H., Travi, Y., Blavoux, B., 2001. Isotopic typology of the precipitation in the Western Mediterranean Region at three different time scales. Geophys. Res. Lett. 28 (7), 1215–1218. https://doi.org/10.1029/2000gl012407.

Celle-Jeanton, H., Travi, Y., Loye-Pilot, M.-D., Huneau, F., Bertrand, G., 2009. Rainwater chemistry at a Mediterranean inland station (Avignon, France): local contribution versus long-range supply. Atmos. Res. 91, 118–126. https://doi.org/10.1016/j.atmosres.2008.06.003.

Celle, H., 2000. Caractérisation des précipitations sur le pourtour de la Méditerranée occidentale – approche isotopique et chimique. Ph.D. Thesis, pp. 222.

Chandrajith, R., Diyabalanage, S., Premathilake, K.M., Hanke, C., van Geldern, R., Barth, J.A.C., 2016. Controls of evaporative irrigation return flows in comparison to seawater intrusion in coastal karstic aquifers in northern Sri Lanka: evidence from solutes and stable isotopes. Sci. Total Environ. 548–549, 421–428. https://doi.org/10.1016/j.scitotenv.2016.01.050.

Cimino, A., Abbate, R., Tusa, A.M., 1998. The regional park of the Nebrodi Mts. (Sicily): a contribution to an integrated groundwater management. Environ. Geol. 34, 320–328.

Clark, I.D., Fritz, P., 1997. Environmental Isotopes in Hydrogeology. CRC Press, pp. 348.

Craig, H., 1961. Isotopic variations in meteoric waters. Science 133, 1702–1703.

Dansgaard, W., 1964. Stable isotopes in precipitation. Tellus 16, 436–468. https://doi.org/10.1111/j.2153-3490.1964.tb00181.x.

Dazy, J., Drogue, C., Charmanidis, P., Darlet, C., 1997. The influence of marine inflows on the chemical composition of groundwater in small islands: the example of the Cyclades (Greece). Environ. Geol. 31, 133–141.

de Vries, J.J., Simmers, I., 2002. Groundwater recharge: an overview of processes and challenges. Hydrogeol. J. 10, 5–17. https://doi.org/10.1007/s10040-001-0171-7.

Delin, G.N., Healy, R.W., Lorenz, D.L., Nimmo, J.R., 2007. Comparison of local-to regional-scale estimates of ground-water recharge in Minnesota, USA. J. Hydrol. 334, 231–249.

Dhar, A., Datta, B., 2009. Saltwater Intrusion Management of Coastal Aquifers. I: linked Simulation-Optimization. J. Hydrol. Eng. 14, 1263–1272. https://doi.org/10.1061/(ASCE)HE.1943-5584.0000097.

Dingman, S.L., 2002. Water in Soils: infiltration and Redistribution. Physical Hydrology. Upper Saddle River. Prentice-Hall, Incpp, New Jersey.

Dörfliger, N., Ferrandini, J., Ferrandini, M., Mathieu, F., 2002. Caractérisation géométrique et hydrodynamique du causse de Bonifacio (Corse) à partir d'une synthèse des connaissances géologiques et hydrogéologiques et par méthodes géophysiques., BRGM/RP-51860-FR. DOI:BRGM/RP-51860-FR.

Eriksson, E., Khunakasem, V., 1969. Chloride concentration in groundwater, recharge rate and rate of deposition of chloride in the Israel Coastal Plain. J. Hydrol. 7, 178–197. https://doi.org/10.1016/0022-1694(69)90055-9.

Famiglietti, J.S., 2014. The global groundwater crisis. Nat. Clim. Change 4, 945–948. https://doi.org/10.1038/nclimate2425.

Fernandez-Chacon, F., Benavente, J., Rubio-Campos, J.C., Kohfahl, C., Jimenez, J., Meyer, H., Hubberten, H., Pekdeger, A., 2010. Isotopic composition (delta O-18 and delta D) of precipitation and groundwater in a semi-arid, mountainous area (Guadiana Menor basin, Southeast Spain). Hydrol. Process. 24, 1343–1356. https://doi.org/10.1002/hyp.7597.

Ferrandini, J., 2003. Chronostratigraphy and paleomagnetism of Oligo-Miocene deposits of Corsica (France): geodynamic implications for the liguro-provencal basin spreading. Bulletin de la Société Géologique de France 174, 357–371. https://doi.org/10.2113/174.4.357.

Florea, L.J., 2013. Selective recharge and isotopic composition of shallow groundwater within temperate, epigenic carbonate aquifers. J. Hydrol. 489, 201–213. https://doi.org/10.1016/j.jhydrol.2013.03.008.

Froehlich, Klaus, Kralik, Martin, Papesch, Wolfgang, Rank, Dieter, Scheifinger, Helfried, Stichler, Willibald, 2008. Deuterium excess in precipitation of Alpine regions – moisture recycling. Isot. Environ. Healt. S. 44, 61–70. https://doi.org/10.1080/10256010801887208.

Garel, E., Santoni, S., Huneau, F., Mayer, A., Travi, Y., Radakovitch, O., Cockenpot, S., Claude, C., 2015. A radium and radon tracing experiment to estimate low submarine groundwater discharge (aquifer of Bonifacio, Corsica, France). In: International Symposium on Isotope Hydrology: Revisiting Foundations and Exploring Frontiers, Vienna, Austria

Gat, J.R., Carmi, I., 1970. Evolution of the isotopic composition of atmospheric waters in the Mediterranean Sea area. J. Geophys. Res. 75, 3039–3048. https://doi.org/10.1029/JC075i015p03039.

Gat, J.R., Carmi, I., 1987. Effect of climate changes on the precipitation patterns and isotopic composition of water in a climate transition zone: case of the Eastern Mediterranean Sea area, The influence of climate change and climatic variability on the hydrologic regime and water resources. Int. Ass. Hydrol. Sci. Public. Vancouver, 513–523.

Gattacceca, J., Deino, A., Rizzo, R., Jones, D.S., Henry, B., Beaudoin, B., Vadeboin, F., 2007. Miocene rotation of Sardinia: new paleomagnetic and geochronological constraints and geodynamic implications. Earth Planet. Sci. Lett. 258, 359–377. https://doi.org/10.1016/j.epsl.2007.02.003.

Ghiglieri, G., Carletti, A., Pittalis, D., 2012. Analysis of salinization processes in the coastal carbonate aquifer of Porto Torres (NW Sardinia, Italy). J. Hydrol. 432, 43–51. https://doi.org/10.1016/j.jhydrol.2012.02.016.

Ghiglieri, G., Carletti, A., Pittalis, D., 2014. Runoff coefficient and average yearly natural aquifer recharge assessment by physiography-based indirect methods for the island of Sardinia (Italy) and its NW area (Nurra). J. Hydrol. 519, 1779–1791. https://doi.org/10.1016/j.jhydrol.2014.09.054.

Gleeson, T., Wada, Y., Bierkens, M.F.P., van Beek, L.P.H., 2012. Water balance of global aquifers revealed by groundwater footprint. Nature 488, 197–200. https://doi.org/10.1038/nature11295.

Gröning, M., Lutz, H.O., Roller-Lutz, Z., Kralik, M., Gourcy, L., Pöltenstein, L., 2012. A simple rain collector preventing water re-evaporation dedicated for δ18O and δ2H analysis of cumulative precipitation samples. J. Hydrol. 448–449, 195–200. https://doi.org/10.1016/j.jhydrol.2012.04.041.

Guttman, L., 1947. The Cornell technique for scale and intensity analysis. Educ. Psychol. Measur. 7, 247–279.

Habets, F., Boone, A., Champeaux, J.L., Etchevers, P., Franchisteguy, L., Leblois, E., Ledoux, E., Le Moigne, P., Martin, E., Morel, S., Noilhan, J., Segui, P.Q., Rousset-Regimbeau, F., Viennot, P., 2008. The SAFRAN-ISBA-MODCOU hydrometeorological model applied over France. J. Geophys. Res. Atmosp. 113, D06113. https://doi.org/10.1029/2007JD008548.

Hartmann, A., Gleeson, T., Wada, Y., Wagener, T., 2017. Enhanced groundwater recharge rates and altered recharge sensitivity to climate variability through subsurface heterogeneity. Proc. Natl. Acad. Sci. 114, 2842–2847. https://doi.org/10.1073/pnas.1614941114.

Hendrickx, J., Walker, G., 1997. Recharge from precipitation. Recharge of phreatic aquifers in (semi-) arid areas 19–98.

Huneau, F., Garel, E., Santoni, S., Jaunat, J., Celle-Jeanton, H., 2015. A new network for isotopes in precipitation of Corsica (France). In: International Symposium on Isotope Hydrology, Revisiting Foundations and Exploring Frontiers, IAEA, Vienna, Austria, 11–15 May 2015.

Jaunat, J., Celle-Jeanton, H., Huneau, F., Dupuy, A., Le Coustumer, P., 2013. Characterisation of the input signal to aquifers in the French Basque Country: emphasis on parameters influencing the chemical and isotopic composition of recharge waters. J. Hydrol. 496, 57–70. https://doi.org/10.1016/j.jhydrol.2013.05.026.

Jaunat, J., Dupuy, A., Huneau, F., Celle-Jeanton, H., Coustumer, P.L., 2016. Groundwater flow dynamics of weathered hard-rock aquifers under climate-change conditions: an illustrative example of numerical modeling through the equivalent porous media approach in the north-western Pyrenees (France). Hydrogeol. J. 24, 1359–1373. https://doi.org/10.1007/s10040-016-1408-9.

Javadi, A., Hussain, M., Sherif, M., Farmani, R., 2015. Multi-objective optimization of different management scenarios to control seawater intrusion in coastal aquifers. Water Resour. Manage. 29, 1843–1857. https://doi.org/10.1007/s11269-015-0914-1.

Kessler, D.H., 1965. Estimation of Subsurface water resources in karstic regions (The rate of percolation in Karstland), UNESCO/AVS/NR/IHD/95, Dubrovnik Symposium.

Kinzelbach, W., Aeschbach, W., Alberich, C., Goni, I.B., Beyerle, U., Brunner, P., Chiang, W.H., Rueedi, J., Zoellmann, K., 2002. A survey of methods for groundwater recharge in arid and semi-arid regions. Early warning and assessment Report series, UNEP/DEWA/RS, 2.

Ladouche, B., Aquilina, L., Dörfliger, N., 2009. Chemical and isotopic investigation of rainwater in Southern France (1996–2002): potential use as input signal for karst functioning investigation. J. Hydrol. 367, 150–164. https://doi.org/10.1016/j.jhydrol.2009.01.012.

Lanini, S., Caballero, Y., Seguin, J.-J., Maréchal, J.-C., 2016. ESPERE, a multiple-method Microsoft Excel application for estimating aquifer recharge. Groundwater 54, 155–156.

Lee, S.Y., Dunn, R.J.K., Young, R.A., Connolly, R.M., Dale, P.E.R., Dehayr, R., Lemckert, C.J., Mckinnon, S., Powell, B., Teasdale, P.R., Welsh, D.T., 2006. Impact of urbanization on coastal wetland structure and function. Austral. Ecol. 31, 149–163. https://doi.org/10.1111/j.1442-9993.2006.01581.x.

Lerner, D.N., Issar, A.S., Simmers, I., 1990. Groundwater recharge: a guide to understanding and estimating natural recharge, 8. Heise Hannoverpp.

Lionello, P., Malanotte-Rizzoli, P., Boscolo, R., 2006. Mediterranean Climate Variability. Elsevier, pp. 438.

Liotta, M., Grassa, F., D'Alessandro, W., Favara, R., Candela, E.G., Pisciotta, A., Scaletta, C., 2013. Isotopic composition of precipitation and groundwater in Sicily, Italy. Appl. Geochem. 34, 199–206. https://doi.org/10.1016/j.apgeochem.2013.03.012.

Longinelli, A., Selmo, E., 2003. Isotopic composition of precipitation in Italy: a first overall map. J. Hydrol. 270, 75–88.

Loye-Pilot, M.D., Martin, J., Morelli, J., 1986. Influence of Saharan Dust on the rain acidity and atmospheric input to the mediterranean. Nature 321, 427–428. https://doi.org/10.1038/321427a0.

Manca, F., Capelli, G., Tuccimei, P., 2015. Sea salt aerosol groundwater salinization in the Litorale Romano Natural Reserve (Rome, Central Italy). Environ. Earth Sci. 73, 4179–4190. https://doi.org/10.1007/s12665-014-3704-9.

Martos-Rosillo, S., González-Ramón, A., Jiménez-Gavilán, P., Andreo, B., Durán, J.J., Mancera, E., 2015. Review on groundwater recharge in carbonate aquifers from SW Mediterranean (Betic Cordillera, S Spain). Environ. Earth Sci. 74, 7571–7581. https://doi.org/10.1007/s12665-015-4673-3.

McDonnell, J.J., Sivapalan, M., Vaché, K., Dunn, S., Grant, G., Haggerty, R., Hinz, C., Hooper, R., Kirchner, J., Roderick, M.L., Selker, J., Weiler, M., 2007. Moving beyond heterogeneity and process complexity: A new vision for watershed hydrology. Water Resour. Res. 43, W07301. https://doi.org/10.1029/2006WR005467.

Meixner, T., Manning, A.H., Stonestrom, D.A., Allen, D.M., Ajami, H., Blasch, K.W., Brookfield, A.E., Castro, C.L., Clark, J.F., Gochis, D.J., Flint, A.L., Neff, K.L., Niraula, R., Rodell, M., Scanlon, B.R., Singha, K., Walvoord, M.A., 2016. Implications of Projected Climate Change for Groundwater Recharge in the Western United States. J. Hydrol. 534, 124–138. https://doi.org/10.1016/j.jhydrol.2015.12.027.

Meredith, K.T., Hollins, S.E., Hughes, C.E., Cendón, D.I., Chisari, R., Griffiths, A., Crawford, J., 2015. Evaporation and concentration gradients created by episodic river recharge in a semi-arid zone aquifer: Insights from Cl−, δ18O, δ2H, and 3H. J. Hydrol. 529 (Part 3), 1070–1078. https://doi.org/10.1016/j.jhydrol.2015.09.025.

Merlivat, L., Jouzel, J., 1979. Global climatic interpretation of the deuterium-oxygen 18 relationship for precipitation. J. Geophys. Res. Oceans 84, 5029–5033.
Orsini, J.-B., Ferrandini, J., Ferrandini, M., Loÿe, M.-D., Pluquet, F., Guennoc, P., Thinon, I., Santiago, M., Reynaud, J.-Y., Oggiano, G., Cherchi, G., Gattaccaca, J., Orrù, P., Puliga, G., Pintus, M., Ulzega, A., 2010. Notice explicative, carte géol. France (1/50 000), feuille Sotta-Bonifacio-Santa-Teresa-di-Gallura (1127), in press. BRGM, Orléans, pp. 258.
Oudet, J., Münch, P., Verati, C., Ferrandini, M., Melinte-Dobrinescu, M., Gattacceca, J., Cornée, J.-J., Oggiano, G., Quillévéré, F., Borgomano, J., others,, 2010. Integrated chronostratigraphy of an intra-arc basin: 40 Ar/39 Ar datings, micropalaeontology and magnetostratigraphy of the early Miocene Castelsardo basin (northern Sardinia, Italy). Palaeogeogr. Palaeoclimatol. Palaeoecol. 295, 293–306.
Pachauri, R.K., Allen, M.R., Barros, V.R., Broome, J., Cramer, W., Christ, R., Church, J.A., Clarke, L., Dahe, Q., Dasgupta, P., Dubash, N.K., Edenhofer, O., Elgizouli, I., Field, C.B., Forster, P., Friedlingstein, P., Fuglestvedt, J., Gomez-Echeverri, L., Hallegatte, S., Hegerl, G., Howden, M., Jiang, K., Jimenez Cisneroz, B., Kattsov, V., Lee, H., Mach, K.J., Marotzke, J., Mastrandrea, M.D., Meyer, L., Minx, J., Mulugetta, Y., O'Brien, K., Oppenheimer, M., Pereira, J.J., Pichs-Madruga, R., Plattner, G.K., Pörtner, H.O., Power, S.B., Preston, B., Ravindranath, N.H., Reisinger, A., Riahi, K., Rusticucci, M., Scholes, R., Seyboth, K., Sokona, Y., Stavins, R., Stocker, T.F., Tschakert, P., van Vuuren, D., van Ypserle, J.P., 2014. Climate change 2014: synthesis report. Contribution of working groups I, II and III to the fifth assessment report of the intergovernmental panel on climate change. IPCC, p. 151.
Peel, M.C., Finlayson, B.L., McMahon, T.A., 2007. Updated world map of the Köppen-Geiger climate classification. Hydrol. Earth Syst Sci. Discuss. 4, 439–473.
Penna, D., Stenni, B., Sanda, M., Wrede, S., Bogaard, T.A., Gobbi, A., Borga, M., Fischer, B.M.C., Bonazza, M., Charova, Z., 2010. On the reproducibility and repeatability of laser absorption spectroscopy measurements for delta H-2 and delta O-18 isotopic analysis. Hydrol. Earth Syst. Sci. 14, 1551–1566. https://doi.org/10.5194/hess-14-1551-2010.
Reynaud, J.-Y., Ferrandini, M., Ferrandini, J., Santiago, M., Thinon, I., André, J.-P., Barthet, Y., Guennoc, P., Tessier, B., 2012. From non-tidal shelf to tide-dominated strait: the Miocene Bonifacio Basin, Southern Corsica. Sedimentology 60, 599–623. https://doi.org/10.1111/j.1365-3091.2012.01352.x.
Richts, A., Struckmeier, W.F., Zaepke, M., 2011. WHYMAP and the Groundwater Resources Map of the World 1:25,000,000. In: Jones, J.A.A. (Ed.), Sustaining Groundwater Resources. International Year of Planet. EarthSpringer, Netherlands, pp. 159–173.
Rozanski, K., Sonntag, C., Münnich, K.O., 1982. Factors controlling stable isotope composition of European precipitation. Tellus 34, 142–150.
Santoni, S., Garel, E., Huneau, F., 2016a. Defining a conceptual model for the coastal aquifers of Mediterranean islands, an example from Corsica (France). EGU General Assembly Conference Abstracts 18, 9268.
Santoni, S., Huneau, F., Garel, E., Aquilina, L., Vergnaud-Ayraud, V., Labasque, T., Celle-Jeanton, H., 2016b. Strontium isotopes as tracers of water-rocks interactions, mixing processes and residence time indicator of groundwater within the granite-carbonate coastal aquifer of Bonifacio (Corsica, France). Sci. Total Environ. 573, 233–246. https://doi.org/10.1016/j.scitotenv.2016.08.087.
Santoni, S., Huneau, F., Garel, E., Vergnaud-Ayraud, V., Labasque, T., Aquilina, L., Jaunat, J., Celle-Jeanton, H., 2016c. Residence time, mineralization processes and groundwater origin within a carbonate coastal aquifer with a thick unsaturated zone. J. Hydrol. 540, 50–63. https://doi.org/10.1016/j.jhydrol.2016.06.001.
Scanlon, B.R., Healy, R.W., Cook, P.G., 2002. Choosing appropriate techniques for quantifying groundwater recharge. Hydrogeol. J. 10, 18–39. https://doi.org/10.1007/s10040-001-0176-2.
Scanlon, B.R., Keese, K.E., Flint, A.L., Flint, L.E., Gaye, C.B., Edmunds, W.M., Simmers, I., 2006. Global synthesis of groundwater recharge in semiarid and arid regions. Hydrol. Process. 20, 3335–3370. https://doi.org/10.1002/hyp.6335.
Scozzafava, M., Tallini, M., 2001. Net infiltration in the Gran Sasso Massif of central Italy using the Thornthwaite water budget and curve-number method. Hydrogeol. J. 9 (5), 461–475. https://doi.org/10.1007/s100400100151.
Stigter, T.Y., Nunes, J.P., Pisani, B., Fakir, Y., Hugman, R., Li, Y., Tome, S., Ribeiro, L., Samper, J., Oliveira, R., Monteiro, J.P., Silva, A., Tavares, P.C.F., Shapouri, M., Cancela da Fonseca, L., El Himer, H., 2014. Comparative assessment of climate change and its impacts on three coastal aquifers in the Mediterranean. Reg. Environ. Change 14, S41–S56. https://doi.org/10.1007/s10113-012-0377-3.
Taylor, R.G., Scanlon, B., Döll, P., Rodell, M., Beek, Wada, R.v., Longuevergne, Y., Leblanc, L., Famiglietti, M., Edmunds, J.S., Konikow, M., Green, L., Chen, T.R., Taniguchi, J., Bierkens, M., MacDonald, M.F.P., Fan, A., Maxwell, Y., Yechieli, R.M., Gurdak, Y., Allen, J.J., Shamsudduha, D.M., Hiscock, M., Yeh, K., Holman, P.J.-F., Treidel, I., 2013a. Ground water and climate change. Nat. Clim. Change 3, 322–329. https://doi.org/10.1038/nclimate1744.
Taylor, R.G., Todd, M.C., Kongola, L., Maurice, L., Nahozya, E., Sanga, H., MacDonald, A.M., 2013b. Evidence of the dependence of groundwater resources on extreme rainfall in East Africa. Nat. Clim. Change 3, 374.
Thornthwaite, C.W., 1948. An approach toward a rational classification of climate. Geograph. Rev. 38, 55–94. https://doi.org/10.2307/210739.
Turc, L., 1954. The water balance of soils. Relation between precipitation evaporation and flow. 5, 491–569.
Yousif, M., Geldern, R.v., Bubenzer, O., 2016. Hydrogeological investigation of shallow aquifers in an arid data-scarce coastal region (El Daba'a, northwestern Egypt). Hydrogeol. J. 24, 159–179. https://doi.org/10.1007/s10040-015-1308-4.
Zhang, L., Walker, G.R., 1998. The Basics of Recharge and Discharge. CSIRO, Collingwood, Australiapp.